REVIEW

Basics and Applications of Solid-State Kinetics: A Pharmaceutical Perspective

AMMAR KHAWAM, DOUGLAS R. FLANAGAN

Division of Pharmaceutics, College of Pharmacy, University of Iowa, Iowa City, Iowa

Received 2 June 2005; revised 20 September 2005; accepted 31 October 2005

Published online in Wiley InterScience (www.interscience.wiley.com). DOI 10.1002/jps.20559

ABSTRACT: Most solid-state kinetic principles were derived from those for homogenous phases in the past century. Rate laws describing solid-state degradation are more complex than those in homogenous phases. Solid-state kinetic reactions can be mechanistically classified as nucleation, geometrical contraction, diffusion, and reaction order models. Experimentally, solid-state kinetics is studied either isothermally or nonisothermally. Many mathematical methods have been developed to interpret experimental data for both heating protocols. These methods generally fall into one of two categories: model-fitting and model-free. Controversies have arisen with regard to interpreting solid-state kinetic results, which include variable activation energy, calculation methods, and kinetic compensation effects. Solid-state kinetic studies have appeared in the pharmaceutical literature over many years; some of the more recent ones are discussed in this review.
 J Pharm Sci 95:472–498, 2006
Keywords: solid-state kinetics; homogenous kinetics; heterogeneous kinetics; stability; degradation; desolvation; reaction-order; isothermal; nonisothermal; arrhenius equation

INTRODUCTION

Many transformations may occur when a solid sample is heated, such as: melting, sublimation, polymorphic transformation, or degradation.[1] These solid-state reactions, are quite common in pharmaceutical sciences, especially polymorphic transformations and degradation. Solid-state chemistry has recently gained much interest in pharmaceutical sciences, which renders the topic of solid-state kinetics important. Solid-state reactions have many forms, however, those that involve weight or enthalpic change are of high interest as their kinetics can be studied by thermal analytical methods. Pharmaceutically, many solid-state kinetic studies are either desolvation reactions or polymorphic transformations. Interest in these reactions is increasing as many formulated drugs, including compendial drugs, are solvates; mainly hydrates. Physicochemical stability of solvates is a concern to pharmaceutical scientists since they may convert to an amorphous form upon desolvation while others may become chemically labile. For example, cephradine dihydrate dehydrates and produces an amorphous form that is further oxidized. Other hydrates may change their state of hydration producing forms with different solubility characteristics.[2] Due to the impact of solvates on the development process and drug performance, it is important to know the stability of these solvates. In addition, with many crystal forms of a drug, stability of the marketed

The authors dedicate this review to the memory of Dr. David J.W. Grant who passed away on December 9, 2005. Dr. Grant was an internationally known authority at the University of Minnesota on the solid-state properties of drugs. He will be remembered as a kind, humble, and brilliant scholar.

Correspondence to: Ammar Khawam (Telephone: 319-335-8819; Fax: 319-335-9349;
E-mail: ammar-khawam@uiowa.edu)

Journal of Pharmaceutical Sciences, Vol. 95, 472–498 (2006)

crystal form should be well understood. One recent example of polymorphic instability is ritonavir, which is Abbott's protease inhibitor for human immunodeficiency virus (HIV). It was temporarily withdrawn from the market because of the transformation of the marketed crystal form (Form I) to a more thermodynamically stable and less soluble form (Form II).[3,4] Another classic example is chloramphenicol palmitate, which was reported to exist in more than one crystalline form and one form was found to be as much as seven times more potent therapeutically than other forms.[5] Therefore, the solid-state stability of polymorphic drugs and the kinetics of such transformations is vital information that needs to be evaluated in the development of such drugs or stable dosage forms.

Kinetics in the solid-state bear similarities to those in homogenous phases like solution or gases. In fact, many of the basic mathematical principles are shared among all three phases. However, solid-state reactions differ substantially from those in the homogenous state. These differences include experimental procedures employed for their study and computation methods for analyzing data.

A review of solid-state kinetics has not appeared in the pharmaceutical literature while many such studies have appeared. As several theories and models for solid-state kinetics have been proposed and applied in the last century, it is important to review them so that pharmaceutical scientists can learn the range of models and apply them. Additionally, kinetic software is available from equipment manufacturers or other sources to analyze solid-state kinetic data. There needs to be an understanding of the underlying assumptions and limitations in such software before one can accurately interpret the results generated.

This work aims to review solid-state reaction kinetic concepts and applications for pharmaceutical solids and to assist pharmaceutical scientists in employing these concepts.

SOLID-STATE KINETICS: FROM HOMOGENOUS TO HETEROGENEOUS PROCESSES

Chemical kinetic concepts were originally based on generalizations from empirical studies of homogenous reactions first in the gas phase. These concepts were later applied to solution phase processes and eventually to solid-state reactions. Solid-state kinetic concepts did not develop separately. However, applying these concepts was justified in the solid-state because of similarities to some homogenous reactions. For example, the Arrhenius equation was historically developed empirically, after which theoretical justification for its use was later introduced in gases through the collision theory and in solutions through the transition-state theory. A similar justification was claimed for the use of this equation in solid-state kinetics.[6] Therefore, solid-state kinetics evolved from homogenous kinetic principles. However, applications of these kinetic principles are different because of the differences between solids, solutions, and gases. For example, particle size, interface advance, and geometric shape are variables unique to heterogeneous reactions and have no equivalent in homogenous reactions. Differences between homogenous and heterogeneous kinetics will be highlighted throughout this review.

Rate Laws

There are many types of solid-state reactions; we will focus on reactions that involve a single solid reactant. A reaction that has acquired great interest is that which follows the reaction scheme below:

$$A_{(s)} \rightarrow B_{(s)} + C_{(g)}$$

Pharmaceutically, desolvation is a reaction that obeys the above scheme, it involves the removal of solvent molecules from the crystalline solvate below its melting point (with dehydration being the specific loss of water).[7,8] In desolvation, A is the solvate or hydrate; B is the parent drug, and C is the solvent or water vapor. The rate[9] of the above reaction is often proportional to the concentration of the reactant or products raised to an integer or fractional power according to:

$$\text{Rate} \propto [A]^n \text{ or } \propto ([A]_0 - [B])^n \text{ or } \propto ([A]_0 - [C])^n \quad (1)$$

Where, A_0 is the initial concentration of A, and n, is the order of the reaction. The rate of a reaction is usually studied by following the decrease in reactant concentration or increase in product concentration. Therefore, the reaction rate law becomes:

$$\begin{aligned} \text{Rate} = \frac{d[A]}{dt} = -\frac{d[B]}{dt} = -\frac{d[C]}{dt} = -k[A]^n \\ = k([A]_0 - [B])^n = k([A]_0 - [C])^n \end{aligned} \quad (2)$$

Where, k is the reaction rate constant. If the evolved gas (C) is efficiently flushed such that $C \approx 0$, the above equation reduces to:

$$\text{Rate} = \frac{d[A]}{dt} = -\frac{d[B]}{dt} = -k[A]^n = k([A]_0 - [B])^n \tag{3}$$

If the reaction is an elementary unimolecular ($n = 1$) reaction, the rate law would be (following only the reactant concentration):

$$\text{Rate} = \frac{d[A]}{dt} = -k[A] \tag{4}$$

Which upon integration becomes:

$$-\ln\frac{[A]}{[A_0]} = kt \tag{5}$$

The above expressions use concentration ([A]), which is usually measured in solution kinetics. However, in solid-state kinetics, concentration has little meaning because the sample is not homogenous, hence reactivity is not the same throughout the sample (nonisotropic) and "concentration" does not relate to reactivity. Figure 1 depicts the difference between homogenously (dark spots, Fig. 1a) and heterogeneously distributed reaction sites (dark spots, Fig. 1b). In solids, reactions occur or are initiated at defects in the crystal lattice or at crystal surfaces, edges, or corners.[5]

Ideally, a perfect crystal contains no imperfections (defects) thus having minimal reactivity. However, in reality, perfect crystals are rare and most crystal lattices contain imperfections. Lattice imperfections can be point defects and dislocations. Point defects are defects where units are missing from the lattice leaving "vacancies" in the lattice. These missing units may be atoms, molecules, or ions. Point defects are also generated when foreign atoms or ions (e.g., impurities) occupy normal lattice positions. Dislocations in the lattice structure result during crystal growth due to surface or internal stresses. A dislocation is a discontinuity in the regularity of the lattice that exists in the bulk of a crystal.[10] For example, a group of parallel planes in the lattice could be shifted by a certain lattice spacing, which could be due to rapid crystal growth in which molecules (or ions or atoms) do not have time to reach their lowest energy states. Imperfection sites are energized sites (i.e., have a higher free energy) in which the activation energy for reaction is least, thus explaining why these sites are highly reactive (Figs. 1–8).

Solid-state kinetics can be studied with thermal analytical methods[1,11] by measuring a sample property as it is heated or held at a constant temperature. If a reaction involves weight loss, then weight is followed throughout the reaction and the kinetics are usually studied by thermogravimetry (TGA). Heat (evolved or consumed) is another measurable property that is used for kinetic evaluation using differential scanning calorimetry (DSC) or differential thermal analysis (DTA). Weight loss or heat flow data are converted to a normalized form called conversion fraction (α). The conversion fraction ranges from 0 to 1 and is a measure of reaction progress as a function of time or temperature.

For isothermal thermogravimetric analysis, the conversion fraction at any time is:

$$\alpha = \frac{m_0 - m_t}{m_0 - m_\infty} \tag{6}$$

where, m_0 is the initial sample weight, m_t is the sample weight at time, t, and m_∞ is the final sample weight. Nonisothermally, the conversion fraction at any temperature is:

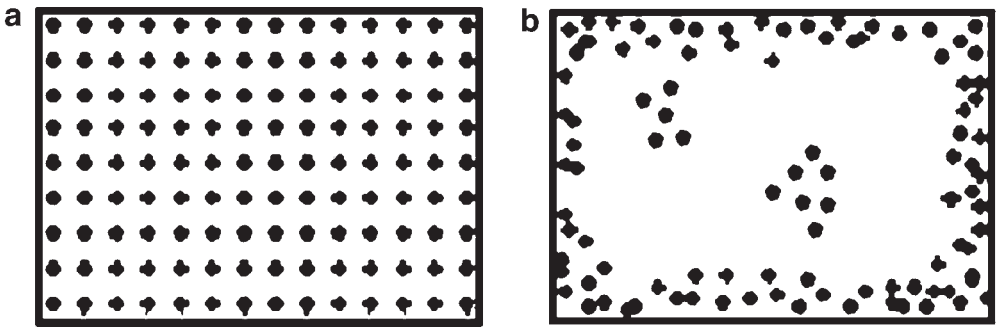

Figure 1. Schematic representation of reactivity (a) homogenous system; (b) heterogeneous system. Black dots represent reaction sites.

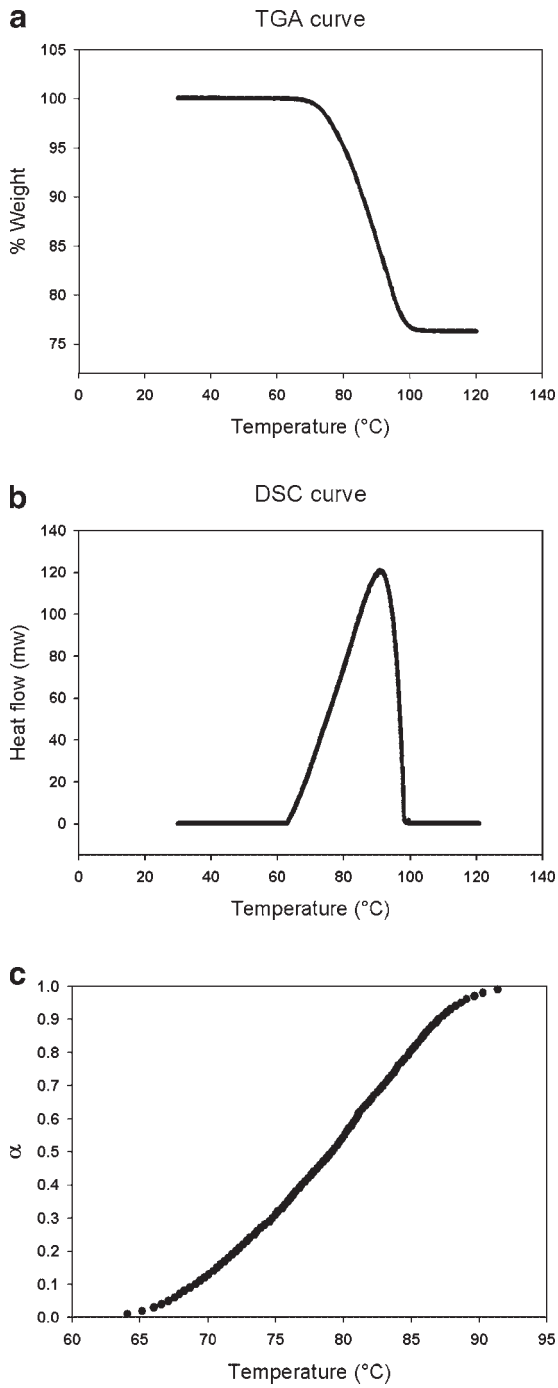

Figure 2. Transformations of TGA and DSC curves to conversion fraction curves: (a, b); Desolvation thermogram of a solid solvate by TGA (a), and DSC (b); (c) α – T plot for the desolvation process for both DSC and TGA results.

$$\alpha = \frac{m_0 - m_T}{m_0 - m_\infty} \tag{7}$$

where, m_T is the sample weight at temperature, T.

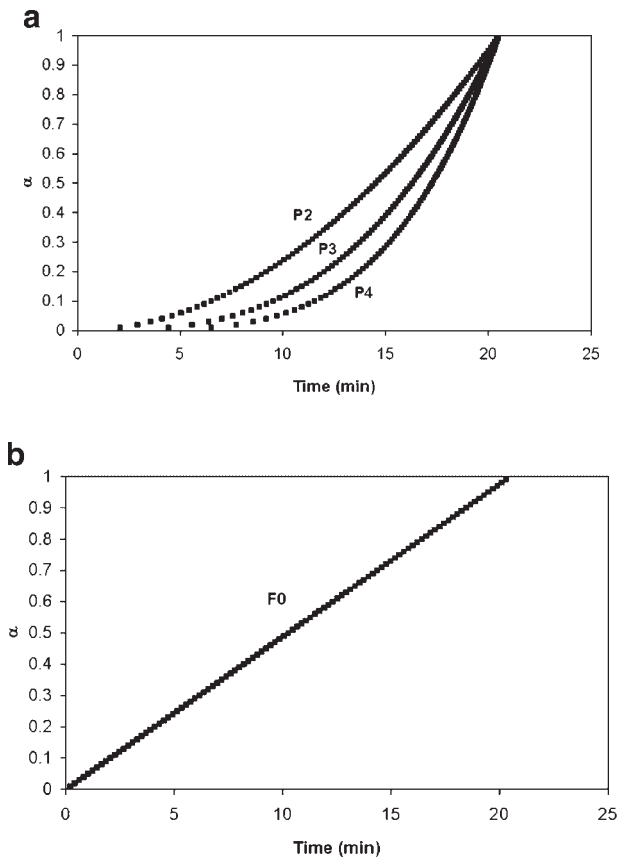

Figure 3. Isothermal α-time plots of different solid-state decomposition models, data simulated for a rate constant of 0.049/min and temperature of 320 K: (a) acceleratory, (b) constant.

For an isothermal DSC/DTA analysis, the conversion fraction[12] at any time is:

$$\alpha = \frac{\mathrm{AUC}_0^t}{\mathrm{AUC}_0^\infty} \tag{8}$$

where, AUC_0^t is the sample peak area from 0 to t and AUC_0^∞ is the total sample peak area. Nonisothermally, the conversion fraction at any temperature can be calculated from:

$$\alpha = \frac{\mathrm{AUC}_0^T}{\mathrm{AUC}_0^\infty} \tag{9}$$

where, AUC_0^T is the sample peak area from 0 to T.

Generally, any analytical method that measures reactant loss or product generation can be converted to α-time (or temperature) plots, transformations of TGA and DSC plots are shown in Figure 2.

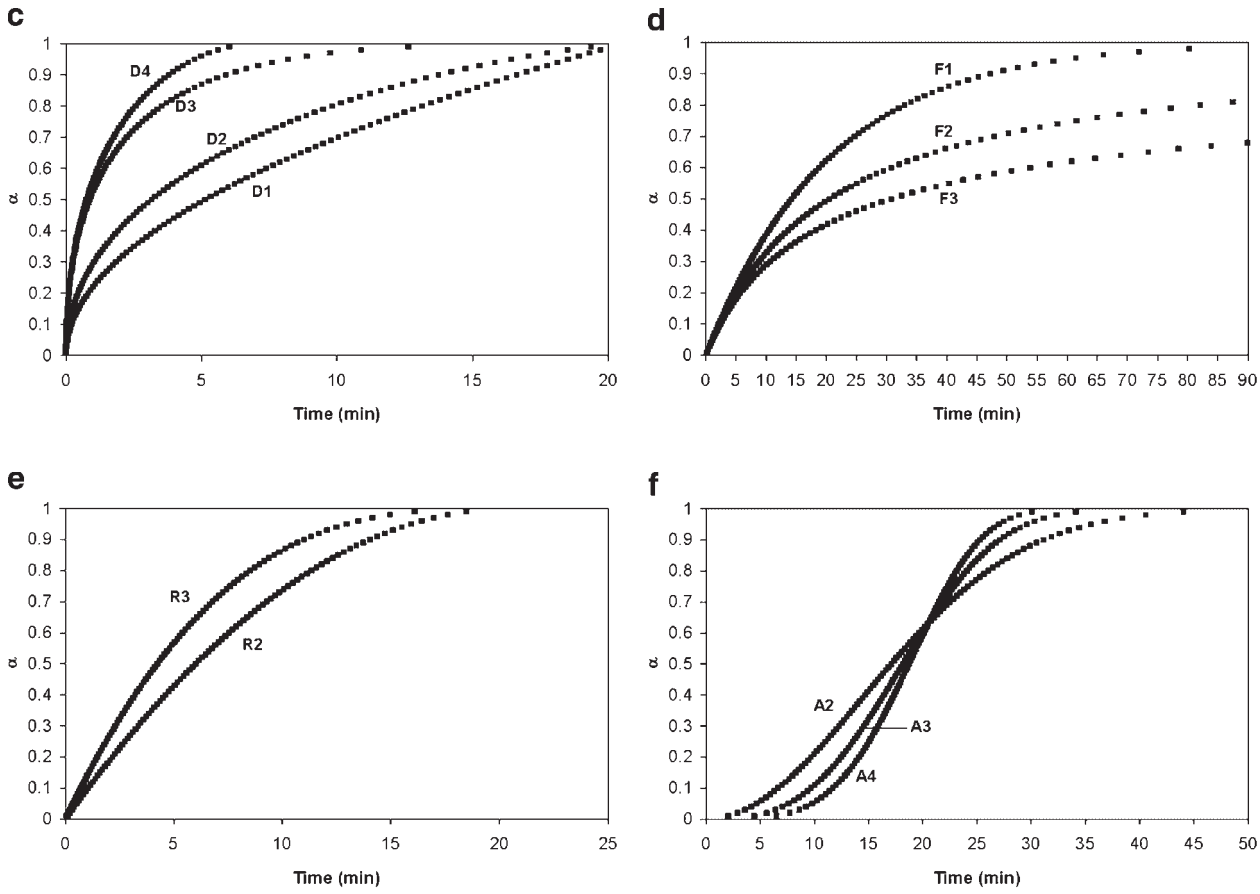

Figure 3. (*Continued*) (c–e) deceleratory, (f) sigmoidal.

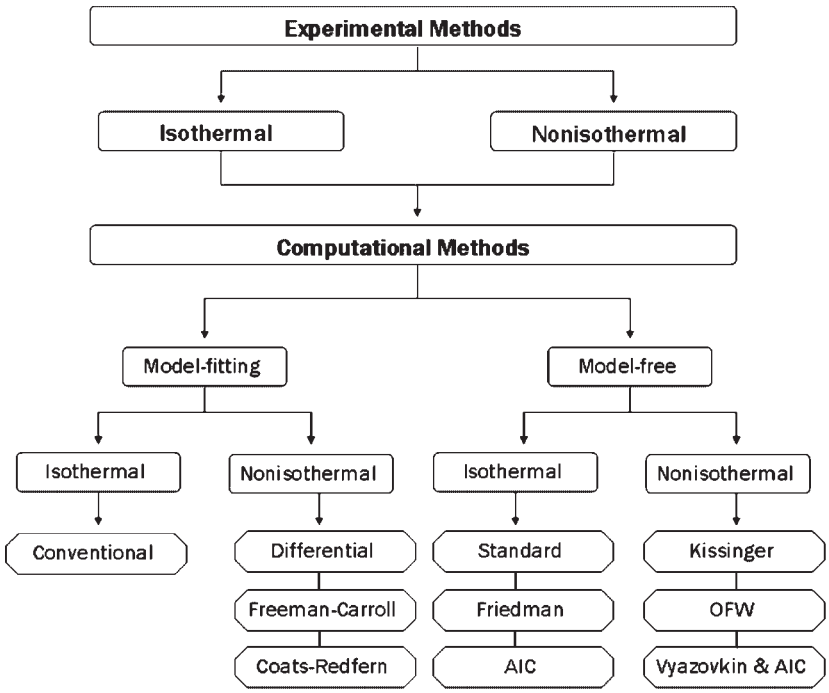

Figure 4. Methods for studying solid-state kinetics.

 DOI 10.1002/jps

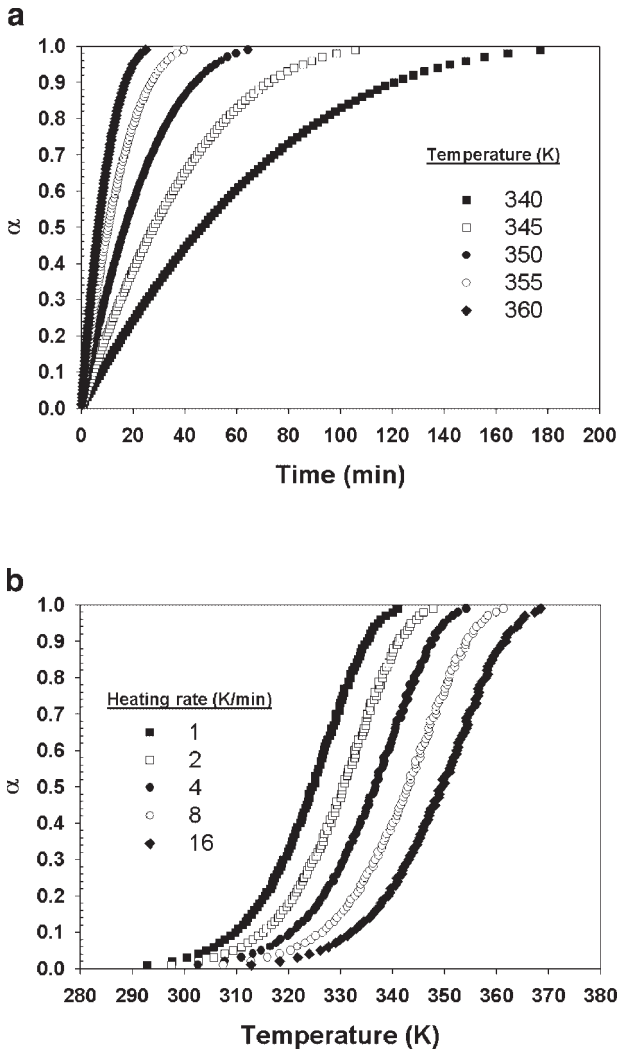

Figure 5. TGA data for a simulated dehydration reaction: (a); isothermal, (b); nonisothermal.

Using the conversion fraction, rate expressions defined in Eqs. 4 and 5 can be written as:

$$\text{Rate} = \frac{d\alpha}{dt} = k(1-\alpha) \tag{10}$$

$$-\ln(1-\alpha) = kt \tag{11}$$

Unlike rate laws in homogenous kinetics, which usually depend on reaction order (i.e., first, second, etc.), a rate law for an elementary solid-state reaction could depend on factors such as rate of nuclei formation, interface advance, diffusion, and/or geometrical shape of solid particles. These factors lead to several decomposition models[13–15] that do not exist in homogenous kinetics and are summarized in Table 1. Eqs. 10 and 11 can be generally expressed as:

$$\frac{d\alpha}{dt} = k f(\alpha) \tag{12}$$

$$g(\alpha) = k t \tag{13}$$

where, $f(\alpha)$ is the differential reaction model and $g(\alpha)$ is the integral reaction model (in some references, $f(\alpha)$ and $g(\alpha)$ definitions may be reversed).

The temperature dependence of the rate constant (k) is usually given by the Arrhenius equation:[16]

$$k = Ae^{-\frac{E_a}{RT}} \tag{14}$$

where, A is the preexponential (frequency) factor, E_a is activation energy, T is absolute temperature, and R is the gas constant. Substitution of Eq. 14 into Eqs. 12 and 13 gives:

$$\frac{d\alpha}{dt} = Ae^{-\frac{E_a}{RT}} f(\alpha) \tag{15}$$

and

$$g(\alpha) = Ae^{-\frac{E_a}{RT}} t \tag{16}$$

MODELS AND MECHANISMS IN SOLID-STATE KINETICS

A model is a theoretical and/or mathematical description of what is observed experimentally. In solid-state reactions, a model describes a reaction and can usually be converted into a mathematical expression (i.e., rate expression). Many models have been proposed for solid-state kinetics, which have been developed based on certain mechanistic assumptions. Therefore, different rate expressions are derived from these models. The models are generally categorized by their underlying mechanistic assumptions or α versus time (α–t) shapes.[13]

Based on the shape of isothermal plots (α–t), models can be classified as, sigmoidal, acceleratory, linear, or deceleratory as seen in Figure 3. Based on the mechanistic assumptions, models are classified as:

A. Nucleation—The rate-limiting step is assumed to be the formation and growth of nuclei, which are finite quantities of product in the reactant lattice. After formation, a nucleus grows and the nucleation rate is different from that of nuclei growth. Nucleation models (A and P models) account for both nucleation and nuclei growth rates.

a

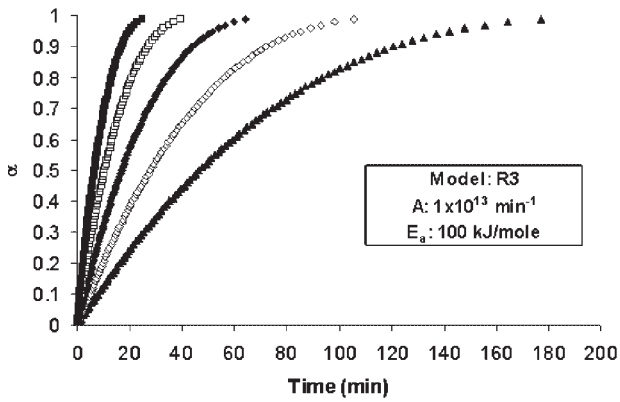

b

α	Temperature (K)				
	340	345	350	355	360
	t (min)	t (min)	t (min)	t (min)	t (min)
0.01	0.75	0.45	0.27	0.17	0.11
0.02	1.51	0.91	0.55	0.34	0.21
.	.	.	.	.	.
.	.	.	.	.	.
.	.	.	.	.	.
0.98	164.44	98.33	59.87	36.87	22.98
0.99	177.04	105.73	64.32	39.63	24.82

α	g(α)				
	A2	A3	.....	R2	R3
0.01	0.10	0.22	.....	0.00	0.00
0.02	0.14	0.27	.....	0.01	0.01
.	.	.	.....	.	.
.	.	.	.....	.	.
.	.	.	.....	.	.
0.98	1.98	1.58	.....	0.89	0.73
0.99	2.15	1.66	.....	0.90	0.78

c

T = 340 K

α	A2		A3		.....	R2		R3	
	g(α)	t (min)	g(α)	t (min)	.....	g(α)	t (min)	g(α)	t (min)
0.01	0.10	0.75	0.22	0.75	.....	0.00	0.75	0.00	0.75
0.02	0.14	1.51	0.27	1.51	.....	0.01	1.51	0.01	1.51
.	.	.	.	.	.....	.	.	.	.
.	.	.	.	.	.....	.	.	.	.
.	.	.	.	.	.....	.	.	.	.
0.98	1.98	164.44	1.58	164.44	.....	0.89	164.44	0.73	164.44
0.99	2.15	177.04	1.66	177.04	.....	0.90	177.04	0.78	177.04
Intercept	0.2990		0.4889		.....	0.0285		0.0001	
Slope (k)	**0.0104**		**0.0072**		.....	**0.0054**		**0.0044**	
r	0.9933		0.9760		.....	0.9966		1.0000	

T = 360 K

α	A2		A3		.....	R2		R3	
	g(α)	t (min)	g(α)	t (min)	.....	g(α)	t (min)	g(α)	t (min)
0.01	0.10	0.11	0.22	0.11	.....	0.00	0.11	0.00	0.11
0.02	0.14	0.21	0.27	0.21	.....	0.01	0.21	0.01	0.21
.	.	.	.	.	.....	.	.	.	.
.	.	.	.	.	.....	.	.	.	.
.	.	.	.	.	.....	.	.	.	.
0.98	1.98	22.98	1.58	22.98	.....	0.89	22.98	0.73	22.98
0.99	2.15	24.82	1.66	24.82	.....	0.90	24.82	0.78	24.82
Intercept	0.2985		0.4885		.....	0.0282		-0.0001	
Slope (k)	**0.0745**		**0.0515**		.....	**0.0387**		**0.0317**	
r	0.9933		0.9761		.....	0.9967		1.0000	

d

	A2		A3		.....	R2		R3	
	ln k	1/T	ln k	1/T	.....	ln k	1/T	ln k	1/T
	ln 0.0104	1/340	ln 0.0072	1/340	.....	ln 0.0054	1/340	ln 0.0044	1/340
	.	.	.	.	.....	.	.	.	.
	.	.	.	.	.....	.	.	.	.
	.	.	.	.	.....	.	.	.	.
	ln 0.0745	1/360	ln 0.0515	1/360	.....	ln 0.0387	1/360	ln 0.0317	1/360
Intercept (ln A)	30.81		30.44		.....	30.15		29.95	
Slope ($-E_a/R$)	-12025.75		-12026.09		.....	-12025.65		-12025.41	
r	-1.0000		-1.0000		.....	-1.0000		-1.0000	
A (min^{-1})	2.40×10^{13}		1.66×10^{13}		.....	1.25×10^{13}		1.02×10^{13}	
E_a (kJ/mol)	100.05		100.06		.....	100.05		100.05	

Figure 6. Isothermal model fitting method (conventional method): (a) simulated α-time curves with 0.25% random error in time at: ▲, 340 K; ♢, 345 K; ◆, 350 K; □, 355 K, and ■, 360 K. Inset shows simulation parameters, (b); tabulated values obtained from the curve in addition to g(α) values for each model, (c); first data fit (g(α) vs. t) for each model and temperature (only two temperature values are shown), (d); second data fit (Arrhenius plot) from which A and E_a can be calculated for each model.

 DOI 10.1002/jps

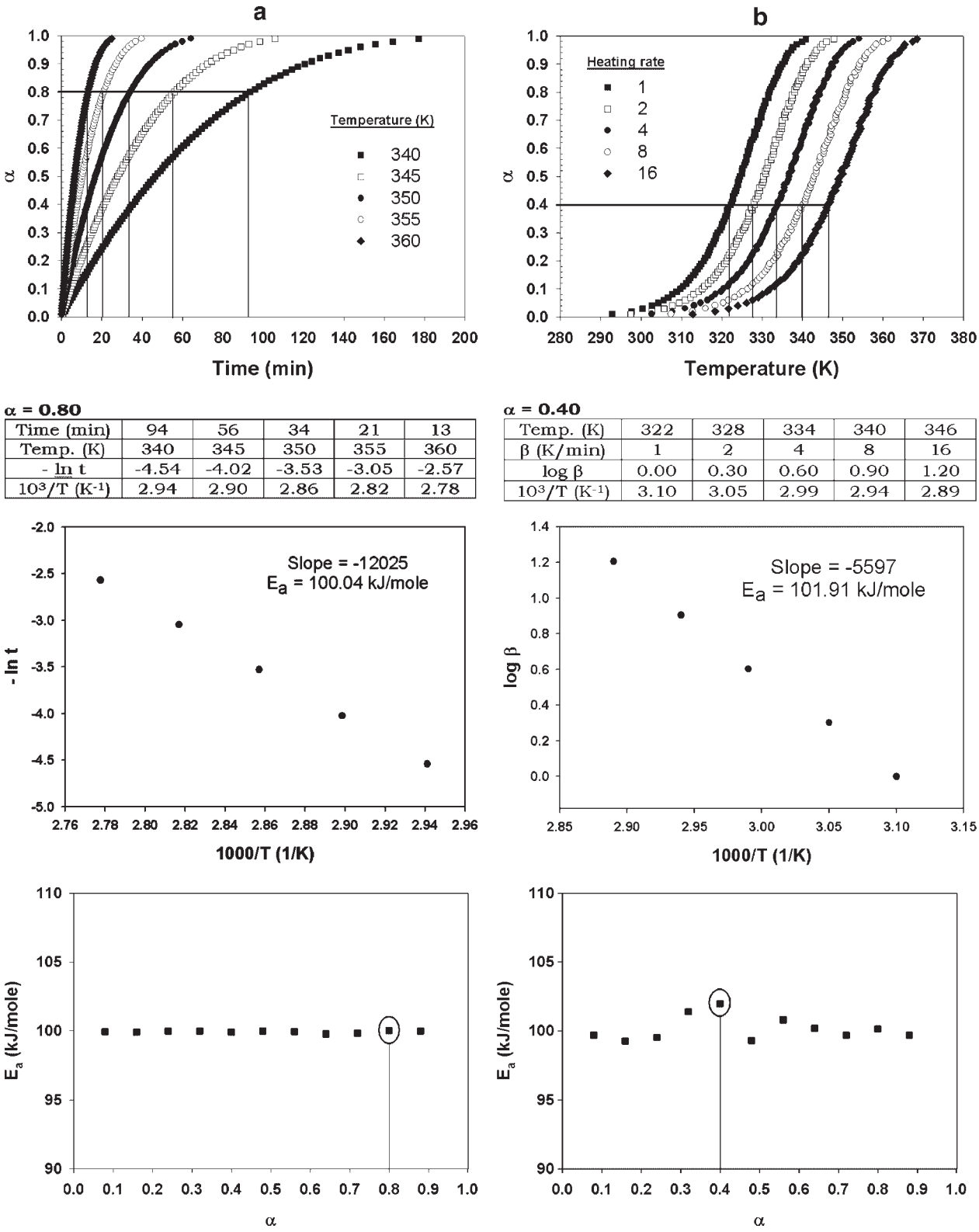

α = 0.80

Time (min)	94	56	34	21	13
Temp. (K)	340	345	350	355	360
- ln t	-4.54	-4.02	-3.53	-3.05	-2.57
$10^3/T$ (K^{-1})	2.94	2.90	2.86	2.82	2.78

α = 0.40

Temp. (K)	322	328	334	340	346
β (K/min)	1	2	4	8	16
log β	0.00	0.30	0.60	0.90	1.20
$10^3/T$ (K^{-1})	3.10	3.05	2.99	2.94	2.89

Figure 7. Isoconversional methods for evaluating solid-state kinetics: (a); Standard method for a set of isothermal curves at: ■, 340 K; □, 345 K; ●, 350 K; ○, 355 K and ◆, 360 K, (b); Ozawa–Flynn–Wall (OFW) method for a set of nonisothermal curves at: ■, 1 K/min; □, 2 K/min; ●, 4 K/min; ○, 8 K/min and ◆, 16 K/min.

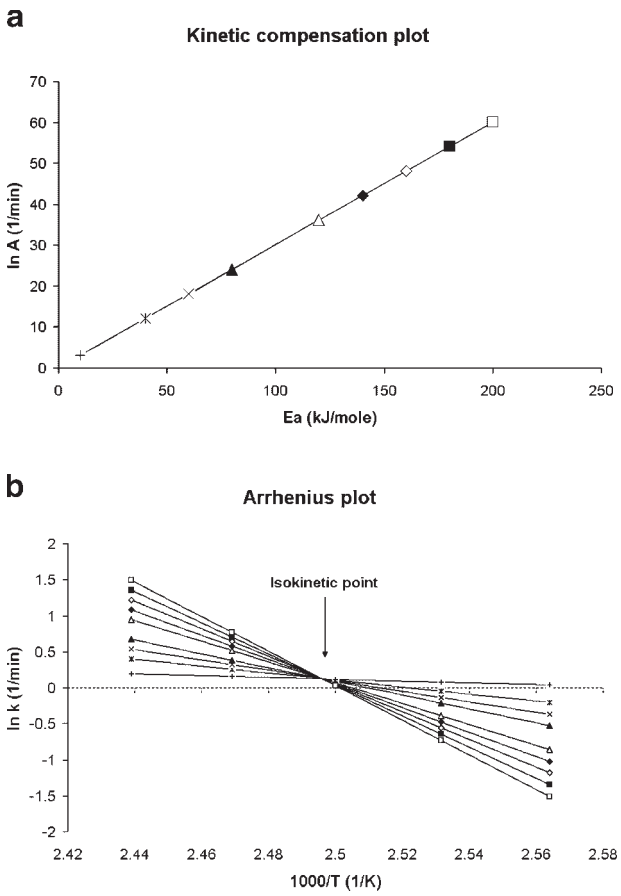

Figure 8. (a). Kinetic compensation effect (KCE), (b). Isokinetic Relationship (IKR). Each point in (a) results from an Arrhenius plot shown in (b).

B. Geometrical contraction—Nucleation is assumed to be instantaneous throughout the surface and the rate-limiting step is the progress of the product layer from the surface of the crystal inward and is different for various crystal morphologies (cubic, cylindrical, spherical, etc.).
C. Diffusion—The rate-limiting step is the diffusion of reactants into reaction sites or products away from reaction sites.
D. Reaction-order—The rate law is based on the reaction order, similar to the same rate expressions in homogenous kinetics.

Sestak and Berggren[17] have suggested a general form for $g(\alpha)$ applicable to all models:

$$g(\alpha) = \alpha^m(1-\alpha)^n(-\ln(1-\alpha))^p \qquad (17)$$

where, m, n, and p are constants for a particular model. Therefore, by assigning particular values to these three terms, any mathematical model can be generated. Table 1 lists the most common models.[13–15]

In homogenous kinetics, when a reaction is studied, the aim of the kinetic study is to obtain kinetic parameters (e.g., rate constants) that can be used to predict product stability. In addition, the mechanism of the reaction is usually investigated. Mechanisms often refer to detailed chemical steps by which a reactant is converted to product(s). In heterogeneous kinetics, the term mechanism usually involves identifying a reaction model, because this information involves chemical steps that are otherwise difficult to obtain experimentally.[11] The choice of a model is generally based on statistical fits of mathematical models to data. However, model selection should also be supported, when possible, by complementary procedures such as microscopy, spectroscopy, X-ray diffraction, product analysis, evolved gas analysis, etc. For example, if nucleation, growth, or gas diffusion are visually observed microscopically, such an observation can support a nucleation or diffusion model obtained from statistical fitting, in addition, conclusions drawn from statistical fitting can be further substantiated by these complementary methods, especially X-ray diffraction.[18]

METHODS FOR STUDYING SOLID-STATE KINETICS

There are many methods used to study solid-state kinetics. These methods can be generally grouped into two categories–experimental and computational; the methods are summarized in Figure 4.

Experimental Methods

There are two approaches utilized to obtain solid-state kinetic data–isothermal and nonisothermal methods. For isothermal methods, samples are studied at several constant temperatures while nonisothermal (dynamic) methods involve heating samples at one or more constant heating rates (usually linear) and following the course of the reaction. Isothermal methods are similar to those used in homogenous kinetics to produce α–time data compared to concentration–time data in homogenous kinetics (Fig. 5). On the other hand, nonisothermal analysis produces α–temperature data (Fig. 5).

Table 1. Solid-State Rate Expressions for Different Reaction Models, Shapes of These Models Is Given in Figure 3

Model	Differential Form[a] $f(\alpha)=\frac{1}{k}\frac{d\alpha}{dt}$	Integral Form[a] $g(\alpha)=kt$
Nucleation models		
Power law (P2)	$2\,\alpha^{(1/2)}$	$\alpha^{(1/2)}$
Power law (P3)	$3\,\alpha^{(2/3)}$	$\alpha^{(1/3)}$
Power law (P4)	$4\,\alpha^{(3/4)}$	$\alpha^{(1/4)}$
Avarami-Erofe'ev (A2)	$2(1-\alpha)[-\ln(1-\alpha)]^{1/2}$	$[-\ln(1-\alpha)]^{1/2}$
Avarami-Erofe'ev (A3)	$3(1-\alpha)[-\ln(1-\alpha)]^{2/3}$	$[-\ln(1-\alpha)]^{1/3}$
Avarami-Erofe'ev (A4)	$4(1-\alpha)[-\ln(1-\alpha)]^{3/4}$	$[-\ln(1-\alpha)]^{1/4}$
Prout–Tompkins (B1)	$\alpha\,(1-\alpha)$	$\ln[\alpha/(1-\alpha)]$
Geometrical Contraction models		
Contracting area (R2)	$2(1-\alpha)^{1/2}$	$[1-(1-\alpha)^{1/2}]$
Contracting volume (R3)	$3(1-\alpha)^{2/3}$	$[1-(1-\alpha)^{1/3}]$
Diffusion models		
1-D diffusion (D1)	$1/2\alpha$	α^2
2-D diffusion (D2)	$[-\ln(1-\alpha)]^{-1}$	$[(1-\alpha)\ln(1-\alpha)]+\alpha$
3-D diffusion-Jander eqn.(D3)	$3(1-\alpha)^{2/3}/2(1-(1-\alpha)^{1/3})$	$[1-(1-\alpha)^{1/3}]^2$
Ginstling–Brounshtein (D4)	$(3/2((1-\alpha)^{-1/3}-1)$	$1-(2\alpha/3)-(1-\alpha)^{2/3}$
Reaction-order models		
Zero-order (F0/R1)	1	α
First-order (F1)	$(1-\alpha)$	$-\ln(1-\alpha)$
Second-order (F2)	$(1-\alpha)^2$	$(1-\alpha)^{-1}-1$
Third-order (F3)	$(1-\alpha)^3$	$0.5\,((1-\alpha)^{-2}-1)$

[a]In some references f(α) and g(α) have opposite designations.

Isothermal Method

This method is based on maintaining samples at several constant temperatures (i.e., isothermal) and as a result, a set of α–time points is produced at each temperature. These methods are based on the isothermal rate equations (Eqs. 13 and 16).

Nonisothermal Method

This method employs a heating rate, usually linear (β), to raise the temperature. A linear heating program follows:

$$T = T_0 + \beta t \tag{18}$$

where, T_0 is the starting temperature, β is the linear heating rate (K/min), and T is the temperature at time, "t". Nonisothermal experiments are usually seen in solid-state kinetics, however, they have been previously applied to the study of homogenous kinetics.[19,20]

The following relationship can be defined for nonisothermal experiments,

$$\frac{d\alpha}{dT} = \frac{d\alpha}{dt} \times \frac{dt}{dT} \tag{19}$$

where, $d\alpha/dT$ is the nonisothermal reaction rate; $d\alpha/dt$ is the isothermal reaction rate and dt/dT is the heating rate (β). Substituting Eq. 15 into Eq. 19 gives,

$$\frac{d\alpha}{dT} = \frac{A}{\beta} e^{-\frac{E_a}{RT}} f(\alpha) \tag{20}$$

Equation 20 represents the differential form of the nonisothermal rate law.

Temperature Integral. Integrating the differential nonisothermal rate law (Eq. 20) produces the integral form of the nonisothermal rate law:

$$g(\alpha) = \frac{A}{\beta} \int_0^T e^{-\frac{E_a}{RT}}\, dT \tag{21}$$

This integral is called the temperature integral and has no analytic solution.[11,21] It has been reported that using nonlinear heating programs such as hyperbolic or parabolic[22] or non-Arrhenius temperature functions of the rate constant[23] leads to exact analytical solutions of the temperature integral. However, this approach has not been widely implemented. To transform the above integral to a more general form found in

mathematical handbooks, the integration variable can be redefined as,

$$\left(x = \frac{E_a}{RT}\right)$$

and the temperature integral then becomes,

$$g(\alpha) = \frac{AE_a}{\beta R}\int_x^\infty \frac{e^{-x}}{x^2}dx \tag{22}$$

If $p(x) = \int_x^\infty \frac{e^{-x}}{x^2}dx$, then Eq. 22 can be written as,

$$g(\alpha) = \frac{AE_a}{\beta R}p(x) \tag{23}$$

where, $p(x)$ is the exponential integral. The main approaches used for evaluating the temperature/exponential integral are:[11]

1. Calculating values of $p(x)$ numerically.
2. Converting $p(x)$ to an approximate form that can be integrated.
3. Approximating $p(x)$ by a series expansion.

The two series most used for approximating the temperature integral are:[1]

I. An asymptotic series expansion

$$p(x) = \frac{e^{-x}}{x^2}\left[1 - \left(\frac{2!}{x}\right) + \left(\frac{3!}{x^2}\right) - \left(\frac{4!}{x^3}\right) + \ldots + (-1)^n\left(\frac{(n+1)!}{x^n}\right) + \ldots\right]$$

II. The Schlömilch series expansion

$$p(x) = \frac{e^{-x}}{x(x+1)}\left[1 - \left(\frac{1}{(x+2)}\right) + \left(\frac{2}{(x+2)(x+3)}\right) - \left(\frac{4}{(x+2)(x+3)(x+4)}\right) + \ldots\right]$$

Many approximations have been reported for the temperature integral,[1,23] two of which will be covered–the Doyle and Senum-Yang approximations. They are among the most frequent temperature/exponential integral approximations as each is the basis of a particular kinetic calculation method.

Doyle Approximation. The Doyle[24–26] approximation of the exponential integral ($p(x)$) is based on the observation that log $p(x)$ is fairly linear with respect to x over a short range of x values. Doyle[24–26] approximated values of $p(x)$ using the first three terms of the Schlömilch series expansion and the observed linear relationship for $x = 28–50$ to obtain by regression the following approximation of the temperature integral:

$$\log p(x) \approx -2.315 - 0.4567x \tag{24}$$

We have determined that the quality of this linear relationship is quite high with an $r^2 = 0.99999$.

Senum-Yang Approximation. Senum and Yang[27] developed an accurate nonlinear approximation of the temperature integral. If variables in Eq. 22 are transformed so that $x = zy$, the integral becomes,

$$g(\alpha) = \frac{AE_a}{\beta Rz}\int_1^\infty \frac{e^{-zy}}{y^2}dy$$

Which can be written as,

$$g(\alpha) = \frac{AE_a}{\beta Rz}E_2(z) \tag{25}$$

$E_2(z)$ or generally, $E_v(z)$ (where v is an integer) is a well known integral[28,29] for $z > 0$ given by the following continued fraction:[30]

$$\frac{E_v(z)}{z} = \frac{e^{-z}}{z}\left(\cfrac{1}{z + \cfrac{v+0}{1 + \cfrac{1}{z + \cfrac{v+1}{1 + \cfrac{2}{z + \cfrac{v+2}{1 + \cfrac{3}{z + \cfrac{v+3}{1 + \cfrac{4}{z + \ldots}}}}}}}}}\right) \tag{26}$$

Truncating the number of terms in the above continued fraction gives the first (one term), second (two terms), third (three terms), and fourth (four terms) degree rational approximation

Table 2. Senum-Yang Approximations of the Temperature Integral

Degree	p(x)
1	$\frac{e^{-x}}{x} \times \frac{1}{(x+2)}$
2	$\frac{e^{-x}}{x} \times \frac{(x+4)}{(x^2+6x+6)}$
3	$\frac{e^{-x}}{x} \times \frac{(x^2+10x+18)}{(x^3+12x^2+36x+24)}$
4[a]	$\frac{e^{-x}}{x} \times \frac{(x^3+18x^2+86x+96)}{(x^4+20x^3+120x^2+240x+120)}$

[a]In Ref. 27, the 4th degree approximation is incorrectly calculated, It is 86× not 88×.

known as the Senum-Yang approximation as given in Table 2.[23,27,31,32]

Calculation Methods

There are two groups of methods used to analyze either isothermal or nonisothermal solid-state kinetic data–model-fitting and model-free methods (Fig. 4).

Model-Fitting Methods

For these methods, different models are fit to the data and the model giving the best statistical fit is chosen as the model of choice from which the activation energy (E_a) and frequency factor (A) can be calculated.

Isothermal Model-Fitting Method (Conventional Method). This method is identical to that in homogenous phase kinetics. It involves two fits: the first, determines the rate constant (k) of the model that best fits the data according to Eq. 13, while the second determines specific kinetic parameters such as the activation energy (E_a) and frequency factor (A) using the Arrhenius equation (Eq. 14). Figure 6 illustrates the application of the conventional method for isothermal model-fitting. Kinetic data were simulated with $E_a = 100$ kJ/mole and $A = 10^{13}$/min and assuming an R3 model with a 0.25% random error in time (Fig. 6a). The upper table in Figure 6b tabulates data from Figure 6a while the lower table calculates $g(\alpha)$ for each reaction model in Table 1. Figure 6c shows the first fit, which determines the model that best fits the data according to Eq. 13. The slope from this fit gives the reaction rate constant and this fitting is repeated for each model at each temperature (only two temperatures are shown in Fig. 6c). For each model, rate constants from all temperatures (five in our simulation) are used for the second fit according to the Arrhenius equation (Eq. 14) as shown in Figure 6d. The frequency factor and activation energy are obtained from the intercept and slope, respectively, of this plot. It is interesting to note that E_a values calculated isothermally by the conventional model-fitting method appear to be equal regardless of the model (i.e., model independent). This behavior does not occur in homogenous kinetic studies where, for example, activation energies obtained from a zero-order fit are substantially different from those obtained by a first, second, or third-order fit. This unusual result has been previously addressed[18,33–35] but without a complete explanation.

Nonisothermal Model-Fitting Methods. There are many model fitting methods that extract the three kinetic parameters known as the kinetic triplet (A, E_a, and model) from nonisothermal data. These methods were used extensively in the early days of solid-state kinetic analysis and they continue to appear. These methods have been critically evaluated[36–40] and it is been shown that the sole use of these methods is not recommended because:

1. They assume a constant kinetic triplet (A, E_a, and model).
2. They involve fitting three parameters (A, E_a, and model), which are simultaneously determined from a single curve.
3. They involve a single heating rate, which is not always sufficient to determine reaction kinetics.

There are a myriad of nonisothermal model fitting methods. However, only a few have been extensively used, which will be discussed below.

Direct differential method. This method[41,42] uses the differential form of the nonisothermal rate law by numerically calculating the differential $\left(\frac{d\alpha}{dT} \approx \frac{\Delta\alpha}{\Delta T}\right)$. Taking the logarithm of the nonisothermal rate law, Eq. 20 gives:

$$\ln \frac{d\alpha/dT}{f(\alpha)} = \ln \frac{A}{\beta} - \frac{E_a}{RT} \qquad (27)$$

Plotting the left-hand side (including the model $f(\alpha)$) versus $1/T$ gives the activation energy (E_a) and frequency factor (A) from the slope and

intercept, respectively. The model that gives the best linear fit is usually chosen as the model.

Freeman–Carroll (Difference-Differential) Method. The Freeman and Carroll method[43,44] is a differential method that was originally developed assuming a reaction-order model ($f(\alpha)=(1-\alpha)^n$). Taking the natural logarithm of the differential form of the nonisothermal rate law (Eq. 20) gives,

$$\ln\frac{d\alpha}{dT}=\ln\frac{A}{\beta}-\frac{E_a}{RT}+\ln f(\alpha) \tag{28}$$

If incremental differences in the variables of Eq. 28 are taken, we obtain:

$$\Delta\ln\frac{d\alpha}{dT}=\Delta\ln f(\alpha)-\frac{E_a}{R}\Delta\frac{1}{T} \tag{29}$$

Which can be rearranged to,

$$\frac{\Delta\ln\frac{d\alpha}{dT}}{\Delta 1/T}=\frac{\Delta\ln f(\alpha)}{\Delta 1/T}-\frac{E_a}{R} \tag{30}$$

or

$$\frac{\Delta\ln\frac{d\alpha}{dT}}{\Delta\ln f(\alpha)}=-\frac{E_a}{R}\frac{\Delta 1/T}{\Delta\ln f(\alpha)} \tag{31}$$

The activation energy can be obtained by plotting the left-hand side of Eqs. 30 and 31 versus $\frac{\Delta\ln f(\alpha)}{\Delta 1/T}$ and evaluating the intercept for Eq. 30 or versus $\frac{\Delta 1/T}{\Delta\ln f(\alpha)}$ and evaluating the slope for Eq. 31.

Coats–Redfern Method. This method[45,46] uses the integral form of the nonisothermal rate law (Eq. 23). Coats and Redfern utilized the asymptotic series expansion for approximating the temperature integral ($p(x)$), producing:

$$\ln\frac{g(\alpha)}{T^2}=\ln\left(\frac{AR}{\beta E_a}\left[1-\left(\frac{2RT_{exp}}{E_a}\right)\right]\right)-\frac{E_a}{RT} \tag{32}$$

where, T_{exp} is the mean experimental temperature.

Plotting the left-hand side (including the model, $g(\alpha)$) of Eq. 32 versus $1/T$ gives the activation energy (E_a) and frequency factor (A) from the slope and intercept, respectively. The model that gives us the best linear fit is chosen as the model. The Coats–Redfern equation was originally derived assuming a first-order model ($g(\alpha)=-\ln(1-\alpha)$) but has been generalized to any reaction model.

Kissinger Method. Kissinger[47,48] proposed a kinetic analysis method for reaction-order models ($f(\alpha)=(1-\alpha)^n$) based on taking the derivative of Eq. 20 generating $d^2\alpha/dT^2$. According to Kissinger, the maximum reaction rate occurs when the second derivative is zero from which the following equation can be obtained:

$$\frac{E_a\beta}{RT_m^2}=A\left(n(1-\alpha)_m^{n-1}\right)e^{-\frac{E_a}{RT_m}} \tag{33}$$

where, T_m is the temperature of the maximum rate and α_m is the conversion value at that rate. The maximum reaction rate represents the peak (i.e., inflection point) of a DSC or DTG curve. Taking the natural logarithm of Eq. 33 and rearranging gives,

$$\ln\frac{\beta}{T_m^2}=\ln\left(\frac{AR\left(n(1-\alpha)_m^{n-1}\right)}{E_a}\right)-\frac{E_a}{RT_m} \tag{34}$$

The activation energy (E_a) is obtained by plotting the left-hand side of the equation versus $1/T_m$ for a series of runs at different heating rates. Eq. 34 has been generalized to any reaction model ($f(\alpha)$).[49]

It is worth noting that the Kissinger method is a model-free method as it does not require any modelistic assumptions to calculate E_a. However, it is not an isoconversional method (discussed below) because it does not calculate E_a values at progressive α values but rather assumes a constant E_a like methods that assume a single E_a value, this method can not detect reaction complexities.[50]

Model-Free/Isoconversional Methods

Model-free methods calculate the reaction activation energy (E_a) without modelistic assumptions, which is usually done by grouping terms such as the frequency factor (A) and model into the intercept of a linear equation and using the slope of that equation to calculate the activation energy (E_a). The frequency factor (A) can be calculated from the intercept of the linear equation but requires modelistic assumptions for such a determination. Therefore, model-free methods usually report only activation energies.

Isoconversional methods are model-free methods that evaluate kinetic parameters, namely the activation energy (E_a) at progressive conversion values (α).[51] These methods require several kinetic curves to perform the analysis and have therefore been called by some as "multicurve" methods[52,53] as shown in Figure 7. Calculations from several curves are performed on the same value of conversion (α), thus the name isoconversional. As a

result, these methods calculate the activation energy for each conversion point ($E_{a\alpha}$), resulting in an isoconversional plot (E_a vs. α) as seen in Figure 7.

The terms, "model-free" and "isoconversional" are sometimes used interchangeably, however, not all model-free methods are isoconversional. For example, the Kissinger method (discussed above) is a model-free method but is not isoconversional.[34] Isoconversional approaches can be used to analyze both isothermal and nonisothermal data as described below.

Isothermal Isoconversional Methods. These methods utilize the isothermal rate law (Eq. 16) and include the standard and Friedman's isoconversional methods.

Standard Isoconversional Method. This method[38,54] can be derived by taking the logarithm of the isothermal rate law (Eq. 16) to give:

$$\ln g(\alpha) = \ln A - \frac{E_a}{RT} + \ln t \tag{35}$$

which can be rearranged to,

$$-\ln t = \ln\left(\frac{A}{g(\alpha)}\right) - \frac{E_a}{RT} \tag{36}$$

A plot of $-\ln t$ versus $1/T$ for each α gives E_a from the slope for that α regardless of the model according to:

$$-\ln t_\alpha = \ln\left(\frac{A}{g(\alpha)}\right)_\alpha - \frac{E_{a\alpha}}{RT_\alpha} \tag{37}$$

Friedman's Isoconversional Method. This method[55] is a differential method and was one of the first isoconversional methods. The logarithm of the isothermal rate law (Eq. 15) gives,

$$\ln\left(\frac{d\alpha}{dt}\right) = (\ln Af(\alpha)) - \frac{E_a}{RT} \tag{38}$$

A plot of $\ln(d\alpha/dt)$ versus $1/T$ at each α gives E_a from the slope for that α regardless of the model according to:

$$\ln\left(\frac{d\alpha}{dt}\right)_\alpha = (\ln Af(\alpha))_\alpha - \frac{E_{a\alpha}}{RT_\alpha} \tag{39}$$

Nonisothermal Isoconversional Methods. Unlike isothermal data, nonisothermal data involve the use of the temperature integral (Eq. 23). Therefore, two common approximations of the temperature integral have been widely used:

1. A linear approximation (less accurate) utilizing the Doyle approximation has been used in the Ozawa and Flynn–Wall methods.
2. A nonlinear approximation (more accurate) utilizing the Senum-Yang approximation has been used in the Vyazovkin method.

Ozawa, Flynn, and Wall (OFW) Method. Ozawa[56] and Flynn–Wall[57] independently developed an isoconversional calculation method for nonisothermal data, which is commonly referred to as the OFW method. Taking the common logarithm of the nonisothermal rate law (Eq. 23) gives the following equation,

$$\log g(\alpha) = \log\frac{AE_a}{\beta R} + \log p(x) \tag{40}$$

Substituting Doyle's approximation (Eq. 24) in Eq. 40 gives,

$$\log g(\alpha) = \log\frac{AE_a}{\beta R} - 2.315 - 0.457x \tag{41}$$

Substituting E_a/RT for x and rearranging gives,

$$\log \beta = \log\frac{AE_a}{g(\alpha)R} - 2.315 - 0.457\frac{E_a}{RT} \tag{42}$$

A plot of $\ln \beta$ versus $1/T$ at each α yields E_a from the slope for that α regardless of the model according to:

$$\log \beta_\alpha = \log\frac{A_\alpha E_{a\alpha}}{g(\alpha)R} - 2.315 - 0.457\frac{E_{a\alpha}}{RT_\alpha} \tag{43}$$

Modified Coats–Redfern Method. Burnham and Braun[58] have transformed the model-fitting Coats–Redfern method to an isoconversional method by rearranging Eq. 32 to:

$$\ln\frac{\beta}{T^2} = \ln\left(\frac{AR}{E_a g(\alpha)}\left[1 - \left(\frac{2RT_{exp}}{E_a}\right)\right]\right) - \frac{E_a}{RT} \tag{44}$$

A plot of $\ln \beta/T^2$ versus $1/T$ at each α yields E_a from the slope for that α regardless of the model according to:

$$\ln\left(\frac{\beta}{T^2}\right)_\alpha = \ln\left(\frac{A_\alpha R}{E_{a\alpha} g(\alpha)}\left[1 - \left(\frac{2RT_{exp}}{E_{a\alpha}}\right)\right]\right) - \frac{E_{a\alpha}}{RT_\alpha} \tag{45}$$

Example of Isoconversional Calculations. Figure 7 depicts the application of two isoconversional methods to simulated kinetic data–isothermal (Fig. 7a–standard method) and nonisothermal (Fig. 7b–Ozawa–Flynn–Wall). The kinetic data were simulated with $E_a = 100$ kJ/mole and $A = 10^{15}$/min and assuming an R3 model in Figure 7a and an F1 model in Figure 7b. Figure 7a shows α-time (α–t) plots while Figure 7b shows α-temperature (α–T) plots. Calculations for each plot (α–t or α–T) were performed for a single conversion value (i.e., isoconversional). This is shown as an isoconversional line with $\alpha = 0.8$ in Figure 7a and $\alpha = 0.4$ for Figure 7b. Values of time (Fig. 7a) or temperature (Fig. 7b) from each isoconversional line are tabulated below each α–t or α–T plots. Plotting the last two rows ($-\ln t$ vs. $10^3/T$ or $\log \beta$ vs. $10^3/T$) of these tables according to Eqs. 37 or 43, respectively, as shown in Figure 7 give Arrhenius-like plots for both isoconversional methods. The activation energy (E_a) is obtained from the slopes of these plots according to Eqs. 37 or 43. The calculated E_a represents a single point ($\alpha = 0.8$ or 0.4) in an isoconversional (E_a–α) plot (circled E_a values in Fig. 7). Repeating this analysis for different α values gives completed isoconversional plots in Figure 7.

Vyazovkin (VYZ) Method. The temperature integral ($p(x)$) in the nonisothermal rate law (Eq. 23) is a function of E_a and temperature. Therefore Eq. 23 can be written as,

$$g(\alpha) = \frac{AE_a}{\beta R} I(E_a, T) \tag{46}$$

where, $I(E_a, T) = p(x)$. The general assumption used in Vyazovkin's[59] method (or any other isoconversional method) is that the reaction model is independent of the heating rate (i.e., $g(\alpha)$ will be the same for any heating rate). Therefore, for a conversion value (α), the relationship below could be defined if two heating rates are applied:

$$g(\alpha) = \frac{A_\alpha E_{a\alpha}}{\beta_1 R} I(E_{a\alpha}, T_{\alpha 1}) = \frac{A_\alpha E_{a\alpha}}{\beta_2 R} I(E_{a\alpha}, T_{\alpha 2}) \tag{47}$$

where, β_1 is the first heating rate, β_2 is the second heating rate, $T_{\alpha 1}$ is the temperature for a particular α using the first heating rate, $T_{\alpha 2}$ is the temperature at the same α using the second heating rate, $E_{a\alpha}$ is the activation energy at that α and A_α is the frequency factor at that α. For an experiment having "n" heating rates, the relationship would be,

$$\frac{A_\alpha E_{a\alpha}}{\beta_1 R} I(E_{a\alpha}, T_{\alpha 1}) = \frac{A_\alpha E_{a\alpha}}{\beta_2 R} I(E_{a\alpha}, T_{\alpha 2}) = \ldots = \frac{A_\alpha E_{a\alpha}}{\beta_n R} I(E_{a\alpha}, T_{an}) \tag{48}$$

which reduces to:

$$\frac{I(E_{a\alpha}, T_{\alpha 1})}{\beta_1} = \frac{I(E_{a\alpha}, T_{\alpha 2})}{\beta_2} = \ldots = \frac{I(E_{a\alpha}, T_{\alpha n})}{\beta_n} = \sigma \tag{49}$$

where, σ is a constant.

For a two heating rate study, using two terms in Eq. 49 we get:

$$\frac{I(E_{a\alpha}, T_{\alpha 1})}{\beta_1} = \frac{I(E_{a\alpha}, T_{\alpha 2})}{\beta_2} = \sigma \tag{50}$$

If both sides are divided by either the right-hand term or left-hand term, we get either:

$$\frac{\beta_2 I(E_{a\alpha}, T_{\alpha 1})}{\beta_1 I(E_{a\alpha}, T_{\alpha 2})} = \frac{\sigma}{\sigma} = 1 \tag{51}$$

or

$$\frac{\beta_1 I(E_{a\alpha}, T_{\alpha 2})}{\beta_2 I(E_{a\alpha}, T_{\alpha 1})} = \frac{\sigma}{\sigma} = 1 \tag{52}$$

Adding Eq. 51 and Eq. 52 gives:

$$\frac{\beta_2 I(E_{a\alpha}, T_{\alpha 1})}{\beta_1 I(E_{a\alpha}, T_{\alpha 2})} + \frac{\beta_1 I(E_{a\alpha}, T_{\alpha 2})}{\beta_2 I(E_{a\alpha}, T_{\alpha 1})} = 2 \tag{53}$$

For three heating rates a similar equation can be obtained, as shown below:

$$\begin{aligned} &\frac{\beta_2 I(E_{a\alpha}, T_{\alpha 1})}{\beta_1 I(E_{a\alpha}, T_{\alpha 2})} + \frac{\beta_3 I(E_{a\alpha}, T_{\alpha 1})}{\beta_1 I(E_{a\alpha}, T_{\alpha 3})} + \frac{\beta_1 I(E_{a\alpha}, T_{\alpha 2})}{\beta_2 I(E_{a\alpha}, T_{\alpha 1})} \\ &\quad + \frac{\beta_3 I(E_{a\alpha}, T_{\alpha 2})}{\beta_2 I(E_{a\alpha}, T_{\alpha 3})} + \frac{\beta_1 I(E_{a\alpha}, T_{\alpha 3})}{\beta_3 I(E_{a\alpha}, T_{\alpha 1})} \\ &\quad + \frac{\beta_2 I(E_{a\alpha}, T_{\alpha 3})}{\beta_3 I(E_{a\alpha}, T_{\alpha 2})} = 6 \end{aligned} \tag{54}$$

For "n" heating rates, Eqs. 53 and 54 can be generalized as,

$$\sum_{i=1}^{n} \sum_{j \neq i}^{n} \frac{\beta_j I(E_{a\alpha}, T_{\alpha i})}{\beta_i I(E_{a\alpha}, T_{\alpha j})} = n(n-1) \tag{55}$$

or

$$\left(n(n-1) - \sum_{i=1}^{n} \sum_{j \neq i}^{n} \frac{\beta_j I(E_{a\alpha}, T_{\alpha i})}{\beta_i I(E_{a\alpha}, T_{aj})} \right) = 0 \tag{56}$$

 DOI 10.1002/jps

For experimental data, Eq. 56 might not converge, but an $E_{a\alpha}$ which minimizes the left-hand side can be found if the following form is used:

$$\left| n(n-1) - \sum_{i=1}^{n} \sum_{j \neq i}^{n} \frac{\beta_j I(E_{a\alpha}, T_{\alpha i})}{\beta_i I(E_{a\alpha}, T_{aj})} \right| = \Omega \qquad (57)$$

Minimizing Eq. 57 is equivalent to minimizing the following:

$$\Omega = \left| \sum_{i=1}^{n} \sum_{j \neq i}^{n} \frac{\beta_j I(E_{a\alpha}, T_{ai})}{\beta_i I(E_{a\alpha}, T_{aj})} \right| \qquad (58)$$

Minimization of Eq. 58 is equivalent to minimizing Eq. 57 because summations contain pairs of inverse ratios. These inverse ratios can be easily seen in Eqs. 53 and 54 which forces each ratio to a value of "1" during minimization. Vyazovkin used the 3rd or 4th degree Senum-Yang approximation of the temperature integral. According to this method, the activation energy ($E_{a\alpha}$) at each α is the value that minimizes Ω.

Vyazovkin's Modified Isoconversional Method. Vyazovkin[22] modified his isoconversional method to account for random temperature variation. This modified method is not limited to linear heating programs and can be used to analyze kinetics from a nonlinear heating program and also isothermal experiments. A modification was introduced to the nonisothermal rate law (Eq. 21) where the heating rate (β) has been included in the integral to represent a heating function rather than a single temperature ($T(t)$ vs. T). Since the heating function is a time dependent function, the integral was changed from a temperature integral (Eq. 21) to a time integral as shown below:

$$g(\alpha) = A \int_0^t \exp\left(-\frac{E_a}{RT(t)}\right) dt \qquad (59)$$

where, $T(t)$ is the heating program used. For each α, Eq. 59 becomes,

$$(g(\alpha))_\alpha = A_\alpha \int_0^{t_\alpha} \exp\left(-\frac{E_{a\alpha}}{RT(t)}\right) dt \qquad (60)$$

which can be generally expressed as,

$$(g(\alpha))_\alpha = A_\alpha J(E_{a\alpha}, T(t_\alpha)) \qquad (61)$$

where,

$$J(E_{a\alpha}, T(t_\alpha)) = \int_0^{t_\alpha} \exp\left(-\frac{E_{a\alpha}}{RT(t)}\right) dt$$

This method allows for use of linear (Eq. 18) and nonlinear heating programs and also can be used for isothermal analysis ($\beta = 0$, $T(t) = T_i$ according to Eq. 18). For any heating program, the integral can be numerically evaluated using the trapezoidal method.

Using the same procedures that were employed for obtaining Eq. 58, it can be shown that all values of $g(\alpha)$ from Eq. 61 are equal, therefore, all $J(E_{a\alpha}, T(t_\alpha))$ values are equal. Thus, equating $J(E_{a\alpha}, T(t_\alpha))$ values and using the same logic as for Eqs. 47–58, we obtain:

$$\Omega = \left| \sum_{i=1}^{n} \sum_{j \neq i}^{n} \frac{J(E_{a\alpha}, T_i(t_\alpha))}{J(E_{a\alpha}, T_j(t_\alpha))} \right| \qquad (62)$$

The activation energy at each α ($E_{a\alpha}$) is the value that minimizes Ω.

Vyazovkin's Advanced Isoconversional (AIC) Method. Vyazovkin[60] introduced a further modification to his isoconversional method. This modification involved integration over smaller time intervals. Therefore, Eq. 60 was altered to give:

$$(g(\alpha))_\alpha = A_\alpha \int_{t_{\alpha-\Delta\alpha}}^{t_\alpha} e^{-\frac{E_{a\alpha}}{RT(t)}} dt \qquad (63)$$

where, $\Delta\alpha = (1/m)$ and m is the number of segments (typically 10–50) into which the integration is divided. Eq. 63 can be generally expressed as,

$$(g(\alpha))_\alpha = A_\alpha J'\lfloor E_{a_\alpha}, T(t_\alpha) \rfloor \qquad (64)$$

As with the methods for obtaining Eqs. 58 and 62, we can obtain:

$$\Omega = \left| \sum_{i=1}^{n} \sum_{j \neq i}^{n} \frac{J'(E_{a\alpha}, T_i(t_\alpha))}{J'(E_{a\alpha}, T_j(t_\alpha))} \right| \qquad (65)$$

As in the previous methods, the activation energy ($E_{a\alpha}$) at each α is the value that minimizes Ω in the above equation. The advanced isoconversional method (AIC) is claimed to be superior to other isoconversional methods[60–62] because integration over smaller time segments can better account for systematic E_a variations.

Complementary Model-Free/Modelistic Approach

Khawam and Flanagan[18] have proposed a complementary approach that uses both model-free and model-fitting methods for kinetic data analysis. This approach utilizes an isoconversional

method (Vyazovkin's) to obtain E_a values, which are compared to values obtained by a model-fitting method (Coats–Redfern). The most accurate model is assumed to be the one, which produces an activation energy closest to that from the isoconversional analysis. This approach allows one to select models that might otherwise be indistinguishable based on quality of regression fit alone. Therefore, the strengths of both methods are used in the evaluation of solid-state kinetics to obtain A and E_a values as well as the best model.

CONTROVERSIES IN SOLID-STATE KINETICS

Discussions over solid-state kinetic studies have caused numerous debates and controversies.[63] Disagreements include questioning whether such kinetics have a good theoretical framework,[64,65] as well as critiques of approximations or assumptions used.[66–68] Some of the controversies will be discussed below.

Varying Activation Energy in Solid-State Kinetics

Solid-state kinetics was developed from reaction kinetics in homogenous systems (i.e., gases and liquids). The Arrhenius equation (Eq. 14) relates the rate constant of a simple one-step reaction to the temperature through the activation energy (E_a) and preexponential factor (A). It has been generally assumed that activation energy (E_a) and frequency factor (A) remain constant, however, it has been shown[69–71] in solid-state reactions that these kinetic parameters may vary with the reaction progress (α). This variation can be detected by isoconversional methods. While this variation appears to be in conflict with basic chemical kinetic principles, in reality, it may not be.

Khawam and Flanagan[54,72] have shown that activation energy variation is of two types—a true variation that results from the complex nature of the solid-state reaction or an artifactual one resulting from the use of some isoconversional methods.

True Variation in Activation Energy

Many explanations have been suggested for the occurrence of a true variation in activation energy, both in homogenous phases[70] and heterogeneous phases.[73] In the solid-state, a variation in activation energy could be observed for an elementary reaction due to the heterogeneous nature of the solid sample or due to a complex reaction mechanism.

Elementary Reactions. If an elementary reaction shows variable activation energy during its progress, it may be attributed to a systematic change in the reaction kinetics. This is not usual for homogeneous reactions which occur between freely moving, identical reactant molecules with random collisional encounters that are usually unaffected by product formation. However, reacting entities in a solid sample are not isolated but interact strongly with neighboring molecules or particles. Therefore, during such a reaction, reactivity may change due to product formation, crystal defect formation, intracrystalline strain, or other similar effects.[73]

Solid-state reactivity could also be affected by experimental variables that would change the reaction kinetics by affecting heat or mass transfer at a reaction interface. For example, temperature changes could affect the kinetics not only through the rate constant but also by mechanistic changes. Elementary reaction kinetics at one temperature could be different from that at another. Complex reaction kinetics (described below) could vary with temperature due to changes in the contribution of each elementary step[73] or change in the rate-determining step. Purge gas flow rate, is another experimental variable that could affect reactivity when reactions produce or consume gaseous components. A low purge flow rate may not preclude the reversibility of a reaction compared to a higher flow rate, which could reduce the reversibility and cause variability in the apparent activation energy and/or introduce errors in calculated reaction rates.

Complex Reactions. If two or more elementary steps, each having a unique activation energy, affect the rate of product formation, the reaction is usually considered complex.[9] In such a reaction, a change in the activation energy as the reaction progresses would be observed. This change will depend on the contribution of each elementary step, which gives an "effective" activation energy that varies with reaction progress. The effective activation energy can be mathematically derived from the nonisothermal degradation rate law (Eq. 15), by taking the natural logarithm followed by differentiation to give:

$$\frac{\mathrm{d}\ln\frac{\mathrm{d}\alpha}{\mathrm{d}t}}{\mathrm{d}\frac{1}{T}} = -\frac{E_a}{R} \tag{66}$$

From this expression, the activation energy at each conversion ($E_{a\alpha}$) can be obtained. If a reaction is composed of two parallel steps according to the following scheme,

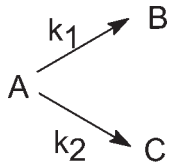

The overall reaction rate is,

$$\frac{d\alpha}{dt} = k_1 f_1(\alpha) + k_2 f_2(\alpha) = A_1 e^{-\frac{E_{a_1}}{RT}} f_1(\alpha) + A_2 e^{-\frac{E_{a_2}}{RT}} f_2(\alpha) \tag{67}$$

Taking the natural logarithm of both sides of Eq. 67 and differentiating gives:

$$\frac{d \ln \frac{d\alpha}{dt}}{d \frac{1}{T}} = -\frac{A_1 E_{a_1} e^{-\frac{E_{a_1}}{RT}} f_1(\alpha) + A_2 E_{a_2} e^{-\frac{E_{a_2}}{RT}} f_2(\alpha)}{R\left(A_1 e^{-\frac{E_{a_1}}{RT}} f_1(\alpha) + A_2 e^{-\frac{E_{a_2}}{RT}} f_2(\alpha)\right)} \tag{68}$$

Since the left-hand side of Eq. 68 is equal to $-(E_a)_{apparent}/R$ (which is also $-(E_a)_\alpha/R$ from Eq. 66), Eq. 68 becomes:

$$E_{a_{apparent}} = E_{a_\alpha} = \frac{A_1 E_{a_1} e^{-\frac{E_{a_1}}{RT}} f_1(\alpha) + A_2 E_{a_2} e^{-\frac{E_{a_2}}{RT}} f_2(\alpha)}{A_1 e^{-\frac{E_{a_1}}{RT}} f_1(\alpha) + A_2 e^{-\frac{E_{a_2}}{RT}} f_2(\alpha)} \tag{69}$$

which can be generalized as:

$$E_{a_\alpha} = \frac{E_{a_1} k_1 f_1(\alpha) + E_{a_2} k_2 f_2(\alpha)}{k_1 f_1(\alpha) + k_2 f_2(\alpha)} \tag{70}$$

Eq. 70 shows that the effective activation energy ($E_{a\alpha}$) is a function of each E_a and α.

Kinetic complexities are not limited to multiple chemical steps. They may also include physical processes that have different activation energies such as:

a. Nucleation and growth—The energy barrier for nucleation could be relatively large compared to growth. Once a nucleus is established, the rate of interface advance can be much lower than that for nucleation. There is no sharp demarcation where nucleation stops and growth starts, since the two are interdependent. The contribution of nucleation may diminish as the reaction progresses, leading to an effective activation energy that varies with the reaction progress.
b. Imperfection distribution—Different samples of the same material may have different imperfection distributions. Therefore, no two solid samples are identical, although they may be similar.[74] This could change the degradation kinetic profiles of each sample.
c. Sublimation along with other reaction processes.
d. Surface adsorption—desorption processes on the reactants/products.
e. Diffusion of a gaseous product through the sample.
f. Rate of growth may vary along each crystallographic axis of a nucleus.[71]
g. Particle size—If a solid-state reaction occurs at surfaces or defect points, larger particles, which have a lower specific surface area, will be less reactive than smaller particles. Various particle sizes could have different kinetic behavior, therefore, a variable particle-sized sample could show complex reaction behavior.
h. Particle or solid morphology—Degradation kinetics of a spherical particle or spherical compact could differ from that of a cylindrical one. A nonhomogenous sample that contains several solid shapes may show complex reaction behavior.
i. Localized melting—Melt degradation rates usually differ from that of the solid producing variable reactivity throughout the sample.[73]

Artifactual Variation in Activation Energy

Isoconversional methods, use several TGA or DSC data sets for kinetic analysis. Some of these methods are sensitive to experimental variables such that changes in these variables produces errors in calculated kinetic parameters like activation energy. When performing isothermal experiments, care should be taken to insure that every run is done under the same experimental conditions (i.e., sample weight, purge rate, sample size distribution, particle morphology, etc.) so that temperature is the only variable for each run. Experimental variation can be minimized, but not totally eliminated. For example, sample mass may vary from one run to the next and affect a reaction because,[75]

1. Larger masses cause larger endothermic or exothermic (self-heating or self-cooling) effects, producing larger deviations from the programmed linear heating rate.

2. Diffusion rates through the sample will change; gaseous diffusion is faster through a lower mass compared to a higher mass.
3. Thermal gradients through the sample might vary, especially when a powder has a low thermal conductivity; larger samples could contain regions where the temperature differs significantly from other regions.

Similarly, sample packing could affect solid reaction kinetics where loosely packed powders contain air pockets that can reduce thermal conductivity or trap evolved gasses compared to a more densely packed powder which would minimize these problems. If any of the above effects occur, a thermogram can be altered such that it falls above or below the expected thermogram for isothermal studies. This would introduce errors in the calculated kinetic parameters obtained from some isoconversional methods.

Temperature Dependence of the Rate Constant

The temperature dependence of the rate constant is almost universally expressed by the Arrhenius equation. However, historically, there was controversy surrounding the temperature dependence of rate constants with many workers proposing several forms for rate constant temperature dependency, as summarized in Table 3. These equations were empirically derived based on quality of fit. Selecting an equation because it gives a reasonable fit to the data is not a sufficient reason for its acceptance, as most of the cited equations will reasonably represent the same experimental data. This occurs because kinetic studies are most often conducted in a narrow temperature range, which makes $1/T$, T, and $\ln T$ (i.e., independent variables in these equations) linearly related to one another. As kinetics developed, most of these equations except, for that of Arrhenius, disappeared because they were theoretically unsound.[16] As a result, the controversy over temperature dependency was finally put to rest, but the controversy and confusion surrounding reaction rate temperature dependence still affect researchers in heterogeneous kinetics.[67,76–81]

Table 3. Summary of Temperature Dependencies of Rate Constants[16]

Equation[a]	Year	Reference[b]
$k = A'F^T(1 + G'T)$	1850	Wilhelmy
$k = Ae^{DT}$	1862	Berthelot
$k = a' + b'T^2$	1881	Warder
$k = Ae^{-\frac{(B-DT^2)}{T}}$	1883	Schwab
$k = Ae^{-\frac{B}{T}}$	1889	Arrhenius
$k = AT^Ce^{-\frac{B}{T}}$	1893	Kooij
$k = AT^C$	1895	Harcourt and Esson
$k = AT^Ce^{-\frac{(B-DT^2)}{T}}$	1898	Van't Hoff

[a] $A, A', B, C, D, F, G', a'$, and b' are temperature independent constants.
[b] Ref. 16 cites the original articles for these expressions.

Galwey and Brown[6] have shown that use of the Arrhenius equation in heterogeneous kinetics is conceptually sound and theoretically well founded. However, use of the Arrhenius equation in nonisothermal experiments is problematic because the temperature integral has no analytical solution. Use of the temperature integral can be avoided by performing kinetic studies isothermally, or using the differential form of the rate law.[23] However, with our current computational tools, approximating the temperature integral is no longer a serious problem because the approximations can be as exact as the kinetic data demands.

Kinetic Compensation Effect

A kinetic compensation effect (KCE)[82–84], is a relationship between the activation energy (E_a) and frequency factor (A) according to:

$$\ln A = bE_a + c \tag{71}$$

where, b and c are constants. This relationship is called a "compensation" because a change in the activation energy (E_a) is partially or completely compensated by a change in the frequency factor (A). KCEs have been classified into three types:[84,85]

a. Type-1—Occurs from a difference in the physicochemical properties of the sample, which includes groups of different but related reactions. For example, groups of reactants that have different substitutions on the same parent molecule, or different crystalline reactants of the same compound containing different defects and impurities.[85]
b. Type-2—Occurs from a difference in the experimental conditions applied to a particular reactant's kinetic studies which includes different atmospheres, sample masses, heating rate, etc.
c. Type-3—Occurs by using different computational methods for kinetic analysis of the

same data set. The significance of this type of compensation has been questioned and is considered a mathematical artifact.[84,85] Garn[76–80] considered that this effect results from using the Arrhenius equation.

Graphically, each Arrhenius plot (ln k vs. $1/T$) gives a pair of A and E_a values. Several Arrhenius plots for a series of reaction studies will give an equal number of A, E_a pairs that can be used to construct a KCE plot (Fig. 8a). If a KCE exists, then overlaying the Arrhenius curves reveals an isokinetic relationship (IKR)[84] as seen in Figure 8b. The IKR is characterized by a point called the "isokinetic point" where all Arrhenius curves intersect. The rate constant at this point (k_{iso}) is equal for all Arrhenius plots and the temperature at this point is called the "isokinetic temperature" (T_{iso}).

From the Arrhenius equation (Eq. 14) and compensation effect (Eq. 71), the isokinetic point can be determined by,

$$T_{iso} = \frac{1}{Rb} \tag{72}$$

$$\ln k_{iso} = c \tag{73}$$

Vyazovkin and Lesniovich[86] have used an IKR to calculate the frequency factor (A), which cannot be obtained directly from isoconversional methods.

The compensation effect has been widely reported, both in homogenous and heterogeneous reactions.[82] However, it remains an empirical observation and has little theoretical justification. Galwey and Brown[83] have summarized the two extreme positions about the compensation effect—either it is an artifact or it has a real chemical significance. If it has real chemical significance, the Arrhenius relationship's meaning is weakened and some basic principles of chemical kinetics may need to be reformulated.

Analytical Methods

Many questions have been raised about analysis and calculation methods used to study solid-state kinetics[1]. The use of nonisothermal experiments has been criticized in favor of isothermal experiments for two reasons—firstly, temperature is an experimental variable in nonisothermal analyses while it is fixed in isothermal analyses, which reduces the total number of variables; secondly, kinetic parameters obtained by both isothermal and nonisothermal experiments usually are not in agreement. On the other hand, nonisothermal studies are considered more convenient than isothermal studies because a sample is not subjected to a rapid temperature rise to a reaction temperature (i.e., heat-up time)[50] in which reaction could occur but not be measured, thus introducing errors in the analysis. This is especially true if the isothermal temperature is high because some decomposition probably occurs before the fixed temperature study is initiated. It was noted[34,37,50] that the disagreement in results from isothermal and nonisothermal experiments should be expected because each covers a different temperature range and due to the complex nature of solid-state reactions, kinetics at different temperatures could vary. The choice of isothermal or nonisothermal experiments is governed by needs of the study, whether it is desired to study reaction kinetics over a wide temperature range (i.e., up to melting) or if a narrow range is sufficient. Also, the application of such results to predicting solid-state stability of a drug affects the choice of most appropriate reaction conditions.

Calculation methods have also raised many controversies because there are many methods and their range of application and validity is unclear. Results obtained by various calculation methods have often been different, even when applied to the same data set. A critical evaluation of these methods was necessary and was initiated in the ICTAC "kinetic project"[36–40] (described below). However, more work needs to be done to standardize the field of solid-state kinetics experimentally, computationally, and conceptually.

ICTAC KINETIC PROJECT

Solid-state kinetics has been associated with controversies and these issues needed to be addressed scientifically. One such approach was through the establishment of a "kinetic project" by several researchers. A kinetics workshop was held during the 11th International Congress on Thermal Analysis and Calorimetry (ICTAC) in Philadelphia, in August, 1996. One of the suggestions of that workshop was to evaluate the various calculation methods in a consistent and scientific fashion by establishing a global kinetic project. The project distributed kinetic data sets to volunteer participants to perform their data analysis.[87,88] Eight sets of kinetic data consisting

of real and simulated isothermal and nonisothermal experiments were distributed. Experimental data were distributed in six sets for the decomposition of calcium carbonate and ammonium perchlorate under nitrogen and vacuum both isothermally and nonisothermally. Two data sets were simulated isothermally and nonisothermally using two equally-weighted, parallel, first-order reactions ($A_1 = 10^{10}$/min, $E_{a1} = 80$ kJ/mole; $A_2 = 10^{15}$/min, $E_{a2} = 120$ kJ/mole).

The purpose of the project was to evaluate the same data with different calculation methods and make judgments based on the kinetic analysis results. Participants were not limited to any particular calculation method. Many such methods were used to analyze the kinetic data sets including: Ozawa–Flynn–Wall, Kissinger, Friedman, Coats–Redfern, direct differential, and many others. Some of these methods were incorporated in software packages such as: TA-KIN®, NETZSCH® thermokinetics, KINETICS®, and AKTS-TA®.[36]

Results for kinetic calculations showed that similar computational methods were in agreement among different laboratories. Analysis of simulated data showed that isoconversional methods produced results that were in general agreement with E_a values ranging from 80 to 120 kJ/mole; model-fitting results of simulated data gave single E_a values intermediate between the two E_a values used thus did not reveal the kinetic complexity of two parallel pathways.[38] Also the kinetic results for the same reaction under various experimental conditions were different (i.e., comparing nitrogen and vacuum atmospheres for calcium carbonate and ammonium perchlorate).

The main conclusions from this project were that the kinetic description of a process strongly depends on the experimental conditions.[89] In addition, multiheating rate methods should be employed to obtain reliable kinetic descriptions and any kinetic process must be described by the complete kinetic triplet.[37,89]

The project succeeded in bridging differences of data analysis in solid-state kinetics. The project was a first step in "standardizing" solid-state kinetic analysis methods. This project should be further expanded to cover other controversial areas in solid-state kinetics.

PHARMACEUTICAL APPLICATIONS

Solid-state kinetics has not been recently reviewed in the pharmaceutical literature. Early reviews were those by Garrett[90,91], Lachman[92], and Carstensen[93]. Interest has recently increased in pharmaceutical solids, their properties and, in many cases, their degradation, dehydration or transformation kinetics.[94] Several kinetic studies of pharmaceutical solids, which have appeared are described below.

Desolvation Kinetics

Wyandt and Flanagan[95] studied the desolvation kinetics of sulfonamide-ammonia adducts. Several nonisothermal model-fitting methods were evaluated[96], which eventually resulted in the use of the direct differential method. A correlation was found between calculated desolvation activation energies of the solid sulfonamide and its pK_a. Drugs with lower pK_a values where found to have higher activation energies and vice versa. This finding was attributed to an acid-base-type interaction between the sulfonamide (acid) and ammonia (base) in the solid-state. The pK_a of the drug was found to inversely affect the strength of the ammonia-drug interaction, which affected desolvation activation energy.

Zhu and Grant[97] studied the dehydration kinetics of nedocromil magnesium pentahydrate,[98–100] a drug used in the treatment of asthma. Dehydration kinetics was studied isothermally by TGA and nonisothermally using DSC. The conventional model-fitting method was used to analyze isothermal data while the Kissinger method was used for nonisothermal kinetic analysis. Dehydration occurred in two steps where the first step involved loss of four water molecules while the second step involved the loss of a single water molecule. Dehydration kinetic results from isothermal TGA (conventional method) agreed with those from nonisothermal DSC (Kissinger method). The first dehydration step followed the A2 model with $E_a = 70$ kJ/mole (TGA) and 63 kJ/mole (DSC) while the second dehydration step followed the A3 model with $E_a = 121$ kJ/mole (TGA) and 112 kJ/mole (DSC). The higher E_a of the second step suggested that the fifth water molecule was more tightly bound in the crystal. They also investigated the effect of particle size, sample weight and vapor pressure on the stability of the drug hydrates. Dehydration E_a values from DSC increased with increasing particle size and decreasing sample weight for both dehydration steps. Changes in E_a with particle size were attributed to changing the surface area/volume ratio, which could affect dehydration kinetics.

Changes in E_a with sample weight were attributed to self-cooling effects of larger sample masses for the endothermic reaction in addition to the varying sample geometry.

Nonisothermal dehydration kinetics of nedocromil sodium trihydrate was investigated by Zhou et al.[101]. They reported that dehydration occurred in two steps, the first step involved the loss of two water molecules while the second step involved the loss of the third water molecule. They studied dehydration kinetics by DSC and saw by thermomicroscopy that water escaped along the needle axis in the first dehydration step, while this directionality was not observed for the second dehydration step. From isoconversional plots using Vyazovkin's advanced isoconversional (AIC) method, they obtained a conversion range ($0.2 < \alpha < 0.8$) having a relatively constant activation energy (~70 kJ/mole). They then applied a model-fitting method (Coats–Redfern) to analyze data within this conversion range. Their results showed the R1 model to be the best fit for the first dehydration step, however, no model gave a satisfactory fit for the second dehydration step, which had an E_a that varied between 130 and 140 kJ/mole. They suggested that a model-fitting approach alone was insufficient for such kinetic analysis. They also studied the effects of particle size and purge gas flow rate on the dehydration kinetics and found that decreasing particle size had little effect on the E_a value of the first dehydration step while it raised the E_a of the second dehydration step and increased its variability. This abnormal behavior was attributed to formation of coherent particle aggregates from which water escape was impeded. Changing the purge gas flow rate had similar effects on calculated E_a values where lower flow rates (10 mL/min, compared to 70 and 150 mL/min) raised the E_a value and increased E_a variability, especially for the second dehydration step. This behavior was attributed to slower water escape from surface of the solid compared to its center. Finally, they were able to rationize dehydration behavior based on crystal structure where channels were observed through which water molecules could move.

Han and Suryanarayanan[102] studied the influence of temperature and water vapor pressure on the dehydration kinetics of carbamazepine dihydrate, an antiepileptic drug. Dehydration was studied isothermally by TGA, DSC, and powder X-ray diffraction (PXRD). Dehydration kinetic parameters were obtained from TGA data with model-fitting methods. Dehydration kinetics was found to follow the phase boundary model (R2) with an activation energy of about 68 kJ/mole. When water vapor pressure was varied, the degradation model changed from R2 to the A3 model, in some cases, while no model could be fitted to other cases. With the aid of PXRD and DSC, they concluded that dehydration under different water vapor pressures alter the crystallographic form of the drug. They claimed that water vapor pressure can have opposing effects on the rate of dehydration. Increased water vapor pressure can decrease the driving force (i.e., shift the reaction towards the hydrate), reducing the reaction rate. On the other hand, water can function as a plasticizer in the solid and increase molecular mobility, increasing nucleation and reaction rates. The overall dehydration rate is the sum of these two opposing effects of moisture.

Degradation Kinetics

Long et al.[103] have studied the nonisothermal kinetics of anhydrous aspirin degradation in the melt by TGA. They reported that degradation occurs in two steps, first; by formation of linear oligomers of acetylsalicylic acid, which are converted to cyclic oligomers in the second degradation step. Kinetics were analyzed using Vyazovkin's AIC method and showed that the apparent E_a decreases from ~120 kJ/mole ($\alpha = 0.01$) to ~25 kJ/mole ($\alpha = 0.5$) and increases in the second degradation step to ~130 kJ/mole ($\alpha = 0.93$). From the calculated activation energy, they were able to make isothermal kinetic predictions of aspirin's stability at different temperatures. Their predicted time for 5% decomposition at 30°C (~874 days) was similar to the labeled shelf-life determined by the typical stability protocols. By combining thermal analysis and mass spectrometry, they were able to propose a degradation scheme in which aspirin produces acetic acid and linear oligomers of acetylsalicylic acid, which were then converted into cyclic oligomers.[104]

Rodante et al.[105,106] have studied decomposition kinetics of structurally related penicillins by simultaneous TGA-DSC analysis. They conducted both isothermal and nonisothermal experiments and extracted kinetic parameters from each by model-fitting and isoconversional methods. Their results showed that the decomposition of oxacillin and cloxacillin occurs in a single step while that for dicloxacillin, benzylpenicillin, and ampicillin

occur in two steps. Carbenicillin decomposes in three steps. All decompositions were preceded by a dehydration step. They have shown that solid-state penicillin decomposition processes were complex, and such complexity is not revealed isothermally, even when isoconversional methods are employed.

Crystallization Kinetics

Zhou et al.[33] used DSC to study crystallization kinetics of amorphous nifedipine, a calcium channel blocker under both isothermal and non-isothermal conditions. For each condition, kinetic analysis was performed by model-fitting (conventional and Coats–Redfern) and isoconversional (Vyazovkin's AIC) methods. Based on the results of isoconversional methods, model-fitting methods were performed in conversion ranges where the activation energy was relatively constant ($0.05 < \alpha < 0.8$). Isothermal and nonisothermal results from model-free analysis were comparable ($E_a \sim 130$ kJ/mole) and model-fitting methods showed that nifedipine crystallization followed the Avarami-Erofe'ev nucleation (A4) model which transforms to A3 then A2 models as crystallization proceeds.

Umeda et al.[107] studied the polymorphic transition kinetics of tolbutamide (form B to A) and mefenamic acid (Form I to II) isothermally by DSC. Kinetic analysis was performed by a model-fitting method described by Hancock and Sharp.[108] They showed that the polymorphic transition from forms B to A for tolbutamide followed a three-dimensional diffusion model (D3) with an activation energy of about 37 kcal/mole (~156 kJ/mol). Whereas, the polymorphic transition from Forms I to II for mefenamic acid followed a zero-order model (F0) with an activation energy about 86 kcal/mole (~360 kJ/mol).

Kitamura et al.[109] studied the effect of grinding on solid-state stability of cefixime trihydrate an oral cephalosporin antibacterial, using DSC, TGA, and powder X-ray diffraction. Kinetic analysis was performed nonisothermally using the Kissinger method. The dehydration E_a for intact cefixime trihydrate was ~72 kcal/mol (~301 kJ/mole) which was reduced to ~68 kcal/mole (~285 kJ/mole) after a 4-h grinding. They concluded that grinding alters the bonding force between water and cefixime molecules, which was reflected in a decrease in the calculated dehydration activation energy for cefixime trihydrate and therefore, a decrease in its stability.

SUMMARY

We have demonstrated in this review that solid-state reaction kinetics is both a unique and complex area of research.

It is unique because of its significant deviation from homogenous phase kinetic processes. Solid-state kinetics is affected by particle size, crystal defects, crystal strain, and other solid properties not relevant to liquid or gas phase processes. One must carefully interpret solid-state kinetic results and incorporate interpretive caveats that reflect these perturbations. Generalization of such results is at the same time easy and difficult. It is easy because the investigator can use the straight forwarded extrapolation of activation energy, frequency factor and model to other temperatures or conditions. It is difficult because kinetic results can depend upon a myriad of solid-state characteristics making it risky to make such extrapolations without knowing how these factors interact to affect the reaction(s) of interest.

This area is complex because of the mathematical tools and models used to interpret solid-state kinetic data. There is a rich array of kinetic models that arise from the nonisotropic nature of the solid-state. Also, many kinetic studies are carried out under nonisothermal conditions, which further complicates an already complex kinetic picture.

We have attempted to summarize the range of experimental methods (i.e., isothermal and non-isothermal) and the attendant mathematical approaches used to analyze such data. This review has not been exhaustive but rather representative of the common tools and models used. Even though we have focused on reactions involving weight loss (i.e., TGA), many of the tools are applicable to other thermal methods such as DSC. The only requirement is the ability to convert collected data to degree of reaction (α) versus time or temperature.

For the pharmaceutical scientist, our review will hopefully serve as an introduction into the realm of solid-state reaction kinetics. The use of such results to make extrapolations or conclusions about solid drug stability under ambient conditions awaits further development. The question "what can I do with these results?" is presently difficult to answer in a general sense. For specific cases, answers may be generated for narrow applications. Generality in solid-state kinetics of drugs awaits further investigation of the factors affecting such processes and the successful extrapolation to predicting API or formulation stability characteristics.

We hope that this review has narrowed the gap between the thermochemical kinetics and pharmaceutical science worlds. We have cited examples of solid-state kinetic investigations on pharmaceutical solids. Also, we have demonstrated in a pedagogic fashion how collected kinetic data (isothermal or nonisothermal) can be transformed or analyzed to obtain modelistic or model-free results. Finally, pharmaceutical investigators are challenged to have a better understanding of the models, mathematical tools and software they apply to solid-state kinetic reactions.

REFERENCES

1. Brown ME. 1988. Introduction to thermal analysis: techniques and applications. London: Chapman and Hall, pp 127–151.
2. Morris KR. 1999. Structural aspects of hydrates and solvates. In: Brittain HG, editor. Polymorphism in pharmaceutical solids. New York: Marcel Dekker, pp 125–181.
3. Bauer J, Spanton S, Henry R, Quick J, Dziki W, Porter W, Morris J. 2001. Ritonavir: an extraordinary example of conformational polymorphism. Pharm Res 18:859–866.
4. Chemburkar SR, Bauer J, Deming K, Spiwek H, Patel K, Morris J, Henry R, Spanton S, Dziki W, Porter W, Quick J, Bauer P, Donaubauer J, Narayanan BA, Soldani M, Riley D, McFarland K. 2000. Dealing with the impact of ritonavir polymorphs on the late stages of bulk drug process development. Org Process Res Dev 4:413–417.
5. Paul IC, Curtin DY. 1973. Thermally induced organic reactions in the solid state. Acc Chem Res 6:217–225.
6. Galwey AK, Brown ME. 2002. Application of the Arrhenius equation to solid state kinetics: can this be justified? Thermochim Acta 386:91–98.
7. Byrn SR, Pfeiffer RR, Stowell JG. 1999. Solid-state chemistry of drugs, 2nd edn. West Lafayette: SSCI, Inc., pp 279–304.
8. Galwey AK. 2000. Structure and order in thermal dehydrations of crystalline solids. Thermochim Acta 355:181–238.
9. Steinfeld JI, Francisco JS, Hase WL. 1999. Chemical kinetics and dynamics, 2nd edn. Upper Saddle River, NJ: Prentice Hall.
10. Mullin JW. 2001. Crystallization, 4th edn. Oxford: Butterworth-Heinemann, pp 1–31.
11. Brown ME. 2001. Introduction to thermal analysis: techniques and applications, 2nd edn. Amsterdam: Kluwer, pp 181–214.
12. Shah HV, Babb DA, Smith DW, Jr. 2000. Bergman cyclopolymerization kinetics of bis-ortho-diynylarenes to polynaphthalene networks. A comparison of calorimetric methods. Polymer 41:4415–4422.
13. Jacobs PWM, Tompkins FC. 1955. Classification and theory of solid reactions. In: Garner WE, editor. Chemistry of the solid state. New York: Academic Press, pp 184–212.
14. Brown ME, Dollimore D, Galwey AK. 1980. Theory of solid state reaction kinetics. In: Bamford CH, Tipper CFH, editors. Chemical kinetics. Amsterdam: Elsevier, pp 41–72.
15. Galwey AK, Brown ME. 1999. Thermal decomposition of ionic solids: chemical properties and reactivities of ionic crystalline phases. Amsterdam: Elsevier, pp 75–115.
16. Laidler KJ. 1984. The development of the Arrhenius equation. J Chem Educ 61:494–498.
17. Sestak J, Berggren G. 1971. Kinetics of the mechanism of solid-state reactions at increasing temperatures. Thermochim Acta 3:1–12.
18. Khawam A, Flanagan DR. 2005. Complementary use of model-free and modelistic methods in the analysis of solid-state kinetics. J Phys Chem B 109:10073–10080.
19. Zoglio MA, Windheuser JJ, Vatti R, Maulding HV, Jr., Kornblum SS, Jacobs AL, Hamot H. 1968. Linear nonisothermal stability studies. J Pharm Sci 57:2080–2085.
20. Maulding HV, Jr., Zoglio MA. 1970. Flexible nonisothermal stability studies. J Pharm Sci 59: 333–337.
21. Galwey AK, Brown ME. 1999. Thermal decomposition of ionic solids: chemical properties and reactivities of ionic phases. Amsterdam: Elsevier, pp 139–171.
22. Vyazovkin S. 1997. Evaluation of activation energy of thermally stimulated solid-state reactions under arbitrary variation of temperature. J Comput Chem 18:393–402.
23. Flynn JH. 1997. The 'Temperature Integral'—Its use and abuse. Thermochim Acta 300:83–92.
24. Doyle CD. 1961. Kinetic analysis of thermogravimetric data. J Appl Polym Sci 5:285–292.
25. Doyle CD. 1962. Estimating isothermal life from thermogravimetric data. J Appl Polym Sci 6:639–642.
26. Doyle CD. 1965. Series approximations to the equation of thermogravimetric data. Nature 207: 290–291.
27. Senum GI, Yang RT. 1977. Rational approximations of the integral of the Arrhenius function. J Therm Anal 11:445–447.
28. Gautschi W, Cahill WF. 1964. Exponential integral and related functions. In: Abramowitz M, Stegun I, editors. Handbook of mathematical functions with formulas and mathematical tables. Washington, DC: National Bureau of Standards, pp 227–237.

29. Weisstein EW. "Exponential Integral." From MathWorld–A Wolfram Web Resource. http://mathworld.wolfram.com/ExponentialIntegral.html
30. Weisstein EW. "ExpIntegralE." From MathWorld–A Wolfram Web Resource. http://functions.wolfram.com/GammaBetaErf/ExpIntegralE/10/0001/
31. Perez-Maqueda LA, Criado JM. 2000. The accuracy of Senum and Yang's approximations to the Arrhenius integral. J Therm Anal 60:909–915.
32. Urbanovici E, Popescu C, Segal E. 1999. On the accuracy of Senum and Yang's fourth degree rational approximation of the temperature integral. J Therm Anal 55:325–327.
33. Zhou DL, Schmitt EA, Zhang GG, Law D, Vyazovkin S, Wight CA, Grant DJW. 2003. Crystallization kinetics of amorphous nifedipine studied by model-fitting and model-free approaches. J Pharm Sci 92:1779–1792.
34. Vyazovkin S, Wight CA. 1997. Isothermal and nonisothermal reaction kinetics in solids: in search of ways toward consensus. J Phys Chem A 101:8279–8284.
35. Zhou DL, Grant DJW. 2004. Model dependence of the activation energy derived from nonisothermal kinetic data. J Phys Chem A 108:4239–4246.
36. Brown ME, Maciejewski M, Vyazovkin S, Nomen R, Sempere J, Burnham A, Opfermann J, Strey R, Anderson HL, Kemmler A, Keuleers R, Janssens J, Desseyn HO, Li CR, Tang TB, Roduit B, Malek J, Mitsuhashi T. 2000. Computational aspects of kinetic analysis. Part A: the ICTAC kinetics project-data, methods and results. Thermochim Acta 355:125–143.
37. Maciejewski M. 2000. Computational aspects of kinetic analysis. Part B: the ICTAC Kinetics Project—the decomposition kinetics of calcium carbonate revisited, or some tips on survival in the kinetic minefield. Thermochim Acta 355:145–154.
38. Vyazovkin S. 2000. Computational aspects of kinetic analysis. Part C. The ICTAC Kinetics Project—the light at the end of the tunnel? Thermochim Acta 355:155–163.
39. Burnham AK. 2000. Computational aspects of kinetic analysis. Part D: the ICTAC kinetics project—multi-thermal-history model-fitting methods and their relation to isoconversional methods. Thermochim Acta 355:165–170.
40. Roduit B. 2000. Computational aspects of kinetic analysis. Part E: the ICTAC Kinetics Project-numerical techniques and kinetics of solid state processes. Thermochim Acta 355:171–180.
41. Sharp JH, Wentworth SA. 1969. Kinetic analysis of thermogravimetric data. Anal Chem 41:2060–2062.
42. Achar BNN, Brindley GW, Sharp JH. 1966. Int Clay Conf, Jerusalem. 67 p.
43. Freeman ES, Carroll B. 1958. The application of thermoanalytical techniques to reaction kinetics. The thermogravimetric evaluation of the kinetics of the decomposition of calcium oxalate monohydrate. J Phys Chem 62:394–397.
44. Freeman ES, Carroll B. 1969. Interpretation of the kinetics of thermogravimetric analysis. J Phys Chem 73:751–752.
45. Coats AW, Redfern JP. 1964. Kinetic parameters from thermogravimetric data. Nature 201:68–69.
46. Coats AW, Redfern JP. 1965. Kinetic parameters from thermogravimetric data II. J Polym Sci Part B: Polym Lett 3:917–920.
47. Kissinger HE. 1956. Variation of peak temperature with heating rate in differential thermal analysis. J Res Nat Bur Stand 57:217–221.
48. Kissinger HE. 1957. Reaction kinetics in differential thermal analysis. Anal Chem 29:1702–1706.
49. Elder JP. 1985. The general applicability of the Kissinger equation in thermal-analysis. J Therm Anal 30:657–669.
50. Vyazovkin S, Wight CA. 1999. Model-free and model-fitting approaches to kinetic analysis of isothermal and nonisothermal data. Thermochim Acta 341:53–68.
51. Simon P. 2004. Isoconversional methods—fundamentals, meaning and application. J Therm Anal 76:123–132.
52. Zsako J. 1973. Kinetic analysis of thermogravimetric data. VI. Some problems of deriving kinetic parameters from TG curves. J Therm Anal 5:239–251.
53. Zsako J. 1996. Kinetic analysis of thermogravimetric data. XXIX. Remarks on the 'many curves' methods. J Therm Anal 46:1845–1864.
54. Khawam A, Flanagan DR. 2005. Role of isoconversional methods in varying activation energies of solid-state kinetics: I. Isothermal kinetic studies. Thermochim Acta 429:93–102.
55. Friedman HL. 1964. Kinetics of thermal degradation of char-forming plastics from thermogravimetry-application to a phenolic resin. J Polym Sci Part C: Polym Lett 6:183–195.
56. Ozawa T. 1965. A new method of analyzing thermogravimetric data. Bull Chem Soc Jpn 38:1881–1886.
57. Flynn JH, Wall LA. 1966. A quick, direct method for the determination of activation energy from thermogravimetric data. J Polym Sci Part B: Polym Lett 4:323–328.
58. Burnham AK, Braun RL. 1999. Global kinetic analysis of complex materials. Energy Fuels 13: 1–22.
59. Vyazovkin S, Dollimore D. 1996. Linear and nonlinear procedures in isoconversional computations of the activation energy of nonisothermal

reactions in solids. J Chem Inf Comput Sci 36: 42–45.
60. Vyazovkin S. 2001. Modification of the integral isoconversional method to account for variation in the activation energy. J Comput Chem 22:178–183.
61. Budrugeac P, Segal E. 2001. Some methodological problems concerning nonisothermal kinetic analysis of heterogeneous solid-gas reactions. Int J Chem Kinet 33:564–573.
62. Vyazovkin S. 2002. Some confusion concerning integral isoconversional methods that may result from the paper by Budrugeac and Segal "Some methodological problems concerning nonisothermal kinetic analysis of heterogeneous solid-gas reactions". Int J Chem Kinet 34:418–420.
63. Brown ME. 1997. Steps in a minefield—some kinetic aspects of thermal analysis. J Therm Anal 49:17–32.
64. Galwey AK. 2004. Is the science of thermal analysis kinetics based on solid foundations? A literature appraisal. Thermochim Acta 413:139–183.
65. Galwey AK, Brown ME. 2000. Solid-state decompositions—stagnation or progress? J Therm Anal 60:863–877.
66. Galwey AK. 1999. Some misconceptions in the kinetic analyses of pharmaceutical systems. J Pharm Pharmacol 51:879–886.
67. Galwey AK. 2003. Eradicating erroneous Arrhenius arithmetic. Thermochim Acta 399:1–29.
68. Galwey AK. 2003. Perennial problems and promising prospects in the kinetic analysis of non-isothermal rate data. Thermochim Acta 407:93–103.
69. Vyazovkin S, Wight CA. 1997. Kinetics in solids. Annu Rev Phys Chem 48:125–149.
70. Vyazovkin S. 2000. On the phenomenon of variable activation energy for condensed phase reactions. New J Chem 24:913–917.
71. Vyazovkin S. 2000. Kinetic concepts of thermally stimulated reactions in solids: a view from a historical perspective. Int Rev Phys Chem 19: 45–60.
72. Khawam A, Flanagan DR. 2005. Role of isoconversional methods in varying activation energies of solid-state kinetics: II. Nonisothermal kinetic studies. Thermochim Acta 436:101–112.
73. Galwey AK. 2003. What is meant by the term 'variable activation energy' when applied in the kinetic analyses of solid state decompositions (crystolysis reactions)? Thermochim Acta 397: 249–268.
74. Brown ME, Brown RE. 2000. Kinetic aspects of the thermal stability of ionic solids. Thermochim Acta 357-358:133–140.
75. Wendlandt WW. 1986. Thermal analysis, 3rd edn. New York: Wiley. 33 p.
76. Garn PD. 1975. Kinetic compensation effect. J Therm Anal 7:475–478.
77. Garn PD. 1976. The kinetic compensation effect. J Therm Anal 10:99–102.
78. Garn PD. 1978. Kinetic parameters. J Therm Anal 13:581–593.
79. Garn PD. 1988. Kinetics of decomposition of the solid state: is there really a dichotomy? Thermochim Acta 135:71–77.
80. Garn PD. 1990. Kinetics of thermal decomposition of the solid state. II. Delimiting the homogeneous-reaction model. Thermochim Acta 160:135–145.
81. Arnold M, Veress GE, Paulik J, Paulik F. 1981. The applicability of the Arrhenius model in thermal analysis. Anal Chim Acta 124:341–350.
82. Galwey AK. 1977. Compensation effect in heterogeneous catalysis. Adv Catal 26:247–322.
83. Galwey AK, Brown ME. 1997. Arrhenius parameters and compensation behaviour in solid-state decompositions. Thermochim Acta 300:107–115.
84. Koga N. 1994. A review of the mutual dependence of Arrhenius parameters evaluated by the thermoanalytical study of solid-state reactions: the kinetic compensation effect. Thermochim Acta 244:1–20.
85. Brown ME, Galwey AK. 2002. The significance of "compensation effects" appearing in data published in "computational aspects of kinetic analysis": ICTAC project, 2000. Thermochim Acta 387:173–183.
86. Vyazovkin SV, Lesnikovich AI. 1988. Estimation of the pre-exponential factor in the isoconversional calculation of effective kinetic parameters. Thermochim Acta 128:297–300.
87. Brown ME, Maciejewski M, Vyazovkin S. 1997. Kinetics analysis project. Thermochim Acta 307:201–203.
88. Brown ME, Maciejewski M, Vyazovkin S. 1998. Kinetics analysis project. J Therm Anal 51:327–332.
89. Maciejewski M, Reller A. 1987. How (un)reliable are kinetic data of reversible solid-state decomposition processes. Thermochim Acta 110:145–152.
90. Garrett ER. 1962. Prediction of stability of drugs and pharmaceutical preparations. J Pharm Sci 51:811–833.
91. Garrett ER. 1967. Kinetics and mechanisms in stability of drugs. Adv Pharm Sci 2:1–94.
92. Lachman L. 1965. Physical and chemical stability testing of tablet dosage forms. J Pharm Sci 54: 1519–1526.
93. Carstensen JT. 1974. Stability of solids and solid dosage forms. J Pharm Sci 63:1–14.
94. Glass BD, Novak C, Brown ME. 2004. The thermal and photostability of solid pharmaceuticals—a review. J Therm Anal 77:1013–1036.
95. Wyandt CM, Flanagan DR. 1992. Solid-state nonisothermal kinetics of sulfonamide ammonia

adduct desolvation. Thermochim Acta 196:379–389.
96. Wyandt CM, Flanagan DR. 1992. A critical evaluation of three non-isothermal kinetic techniques. Thermochim Acta 197:239–248.
97. Zhu HJ, Grant DJW. 2001. Dehydration behavior of nedocromil magnesium pentahydrate. Int J Pharm 215:251–262.
98. Zhu HJ, Khankari RK, Padden BE, Munson EJ, Gleason WB, Grant DJW. 1996. Physicochemical characterization of nedocromil bivalent metal salt hydrates. 1. Nedocromil magnesium. J Pharm Sci 85:1026–1034.
99. Zhu HJ, Padden BE, Munson EJ, Grant DJW. 1997. Physicochemical characterization of nedocromil bivalent metal salt hydrates. 2. Nedocromil zinc. J Pharm Sci 86:418–429.
100. Zhu HJ, Halfen JA, Young VG, Padden BE, Munson EJ, Menon V, Grant DJW. 1997. Physicochemical characterization of nedocromil bivalent metal salt hydrates. 3. Nedocromil calcium. J Pharm Sci 86:1439–1447.
101. Zhou DL, Schmitt EA, Zhang GGZ, Law D, Wight CA, Vyazovkin S, Grant DJW. 2003. Model-free treatment of the dehydration kinetics of nedocromil sodium trihydrate. J Pharm Sci 92:1367–1376.
102. Han J, Suryanarayanan R. 1998. Influence of environmental conditions on the kinetics and mechanism of dehydration of carbamazepine dihydrate. Pharm Dev Technol 3:587–596.
103. Long GT, Vyazovkin S, Gamble N, Wight CA. 2002. Hard to swallow dry: kinetics and mechanism of the anhydrous thermal decomposition of acetylsalicylic acid. J Pharm Sci 91:800–809.
104. Long GT, Vyazovkin S, Gamble N, Wight CA. 2001. Hard to swallow dry: formation of linear and cyclic oligomers in the anhydrous thermal decomposition of acetylsalicylic acid. J Chem Soc, Perkin Trans 2:436–437.
105. Rodante F, Vecchio S, Tomassetti A. 2002. Multistep decomposition processes for some antibiotics: a kinetic study. Thermochim Acta 394:7–18.
106. Rodante F, Vecchio S, Tomassetti M. 2002. Kinetic analysis of thermal decomposition for penicillin sodium salts—model-fitting and model-free methods. J Pharm Biomed Anal 29:1031–1043.
107. Umeda T, Ohnishi N, Yokoyama T, Kuroda T, Kita Y, Kuroda K, Tatsumi E, Matsuda Y. 1985. Studies on drug nonequivalence. 14. A kinetic-study on the isothermal transition of polymorphic forms of tolbutamide and mefenamic-acid in the solid-state at high-temperatures. Chem Pharm Bull 33:2073–2078.
108. Hancock JD, Sharp JH. 1972. Method of comparing solid-state kinetic data and its application to the decomposition of kaolinite, brucite, and barium carbonate. J Am Ceram Soc 55:74–77.
109. Kitamura S, Miyamae A, Koda S, Morimoto Y. 1989. Effect of grinding on the solid-state stability of cefixime trihydrate. Int J Pharm 56:125–134.